Title
Organ-Level Quorum Sensing Directs Regeneration in Hair Stem Cell Populations

Journal
Cell, 161(2)

ISSN
0092-8674

Authors
Chen, Chih-Chiang
Wang, Lei
Plikus, Maksim V
et al.

Publication Date
2015-04-01

DOI
10.1016/j.cell.2015.02.016

Peer reviewed

Article

Cell

Organ-Level Quorum Sensing Directs Regeneration in Hair Stem Cell Populations

Graphical Abstract

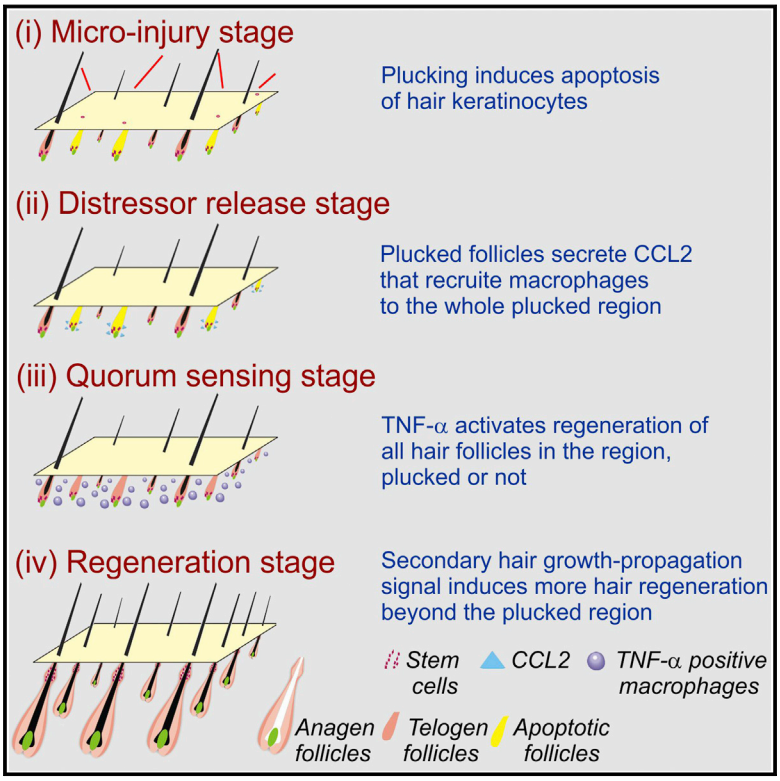

Authors

Chih-Chiang Chen, Lei Wang, ..., Arthur D. Lander, Cheng Ming Chuong

Correspondence

cmchuong@usc.edu

In Brief

Organ-level quorum sensing through a multi-step immune cascade allows collective regeneration of hair follicle populations. This mechanism provides a means to assess the magnitude and extent of injury that the skin has sustained and make an all-or-none decision whether to regenerate.

Highlights

- Quorum sensing underlies collective regenerative behavior in a hair follicle population
- Sensing occurs via injury → CCL2 → macrophage → TNF-α → hair regeneration pathway
- Coupling molecular diffusion and cell mobility achieves a long signaling length scale
- Stem cell social behavior can be exploited to enhance the reliability of regeneration

Accession Numbers

GSE46181

Chen et al., 2015, Cell *161*, 277–290
April 9, 2015
http://dx.doi.org/10.1016/j.cell.2015.02.016

CellPress

Cell

Organ-Level Quorum Sensing Directs Regeneration in Hair Stem Cell Populations

Chih-Chiang Chen,[1,2,3] Lei Wang,[4] Maksim V. Plikus,[5,6,7] Ting Xin Jiang,[1] Philip J. Murray,[8] Raul Ramos,[5,6,7] Christian F. Guerrero-Juarez,[5,6,7] Michael W. Hughes,[9] Oscar K. Lee,[10] Songtao Shi,[11] Randall B. Widelitz,[1] Arthur D. Lander,[5,7,12] and Cheng Ming Chuong[1,3,13,*]

[1]Department of Pathology, University of Southern California, Los Angeles, CA 90033, USA
[2]Department of Dermatology, Taipei Veterans General Hospital, Taipei 112, Taiwan, ROC
[3]Institute of Clinical Medicine and Department of Dermatology, National Yang-Ming University, Taipei, Taiwan 112, ROC
[4]State Key Laboratory of Military Stomatology, Department of Oral and Maxillofacial Surgery, School of Stomatology, The Fourth Military Medical University, Xi'an, Shaanxi 710032, China
[5]Department of Developmental and Cell Biology
[6]Sue and Bill Gross Stem Cell Research Center
[7]Center for Complex Biological Systems
University of California Irvine, Irvine, CA 92697, USA
[8]Division of Mathematics, University of Dundee, Dundee DD1 4HN, UK
[9]International Laboratory of Wound Repair and Regeneration and Institute of Clinical Medicine, National Cheng Kung University, Tainan 701, Taiwan, ROC
[10]Department of Orthopaedics and Traumatology, Taipei Veterans General Hospital, Taipei and Center for Stem Cell Research, National Yang-Ming University and Veterans General Hospital, Taipei 112, Taiwan, ROC
[11]Department of Anatomy and Cell Biology, University of Pennsylvania, School of Dental Medicine, Philadelphia, PA 19104, USA
[12]Department of Biomedical Engineering, University of California Irvine, Irvine, CA 92697, USA
[13]Research Center for Developmental Biology and Regenerative Medicine, National Taiwan University, Taipei 10617, Taiwan
*Correspondence: cmchuong@usc.edu
http://dx.doi.org/10.1016/j.cell.2015.02.016

SUMMARY

Coordinated organ behavior is crucial for an effective response to environmental stimuli. By studying regeneration of hair follicles in response to patterned hair plucking, we demonstrate that organ-level quorum sensing allows coordinated responses to skin injury. Plucking hair at different densities leads to a regeneration of up to five times more neighboring, unplucked resting hairs, indicating activation of a collective decision-making process. Through data modeling, the range of the quorum signal was estimated to be on the order of 1 mm, greater than expected for a diffusible molecular cue. Molecular and genetic analysis uncovered a two-step mechanism, where release of CCL2 from injured hairs leads to recruitment of TNF-α-secreting macrophages, which accumulate and signal to both plucked and unplucked follicles. By coupling immune response with regeneration, this mechanism allows skin to respond predictively to distress, disregarding mild injury, while meeting stronger injury with full-scale cooperative activation of stem cells.

INTRODUCTION

The effective coordination of organ behavior, either under physiological conditions or as a response to injury, is essential for survival. Integration at the level of large-scale organ systems has been extensively studied, but the role of shorter range, local coordination has not. For example, is the regeneration of repeated tissue units within an organ (e.g., hair follicles [HFs] in skin, villi in intestine) coordinated so as to achieve collective decision-making? If so, what are the mechanisms of communication, and how is information integrated? In particular, if injury or malfunction affects only a subset of tissue units in an organ, how is such a collective decision made whether to mount a response that is local (e.g., local repair) or global (e.g., tissue level regeneration)?

Mammalian skin offers an excellent platform to address such questions, because its numerous HFs behave as discrete, repeating, semi-autonomous tissue units (Jahoda and Christiano, 2011) distributed on a 2D plane. HFs undergo cyclic regeneration (Paus et al., 1998) by regulating both intra- and extra-follicular cues for hair stem cell activation (Stenn and Paus, 2001; Plikus et al., 2008, 2011; Festa et al., 2011; Chen and Chuong, 2012), both during physiological regeneration and in response to injury (Chuong et al., 2012). The experimental accessibility of HFs makes them an ideal model to study collective decision making in an organ population in vivo.

Classical studies show that hair plucking produces a micro-injury that can potentially lead to hair regeneration (Collins, 1918; Silver and Chase, 1970). This process is thought to be mediated by an autonomous mechanism in each follicle, in which early apoptosis in the bulge leads to activation of hair germ progenitors (Ito et al., 2002). Here, we uncover evidence that the decision of hair stem cells to be activated or remain quiescent also depends on information coming from neighboring follicles. This possibility was first suggested by our earlier study in which plucking fewer than 50 refractory telogen hairs did not induce hair regeneration, while plucking more than 200 hairs did (Plikus

et al., 2008). Here, by varying the spacing, arrangement, and shapes of plucked regions, we unexpectedly found that plucking 200 hairs, with a proper topological distribution can cause up to 1,200 hairs to regenerate. These results demonstrate marked non-autonomy in HF regeneration and a distinctly non-linear quantitative relationship between plucking and regeneration.

As discussed below, the collective HF response to injury may be seen as an example of quorum sensing, a form of social behavior in which population decisions depend on the density of signaling individuals within a given spatial territory (Bassler, 2002; Pratt, 2005). In order to gain insights into the possible mechanisms underlying this behavior, we first used mathematical modeling to identify the characteristic spatial range over which quorums are sensed, which led us to suspect that the signaling mechanism consists of more than just a diffusible molecule. The time course of molecular changes after plucking, together with the results of genetic and pharmacological manipulation, implicated a two-stage mechanism, involving the release of diffusible signals that recruit immune cells (M1 macrophages) which then actively spread among follicles, where they locally induce regeneration through the release of substances such as Tnf-α.

This work identifies a mechanism for quorum sensing that operates on the millimeter scale to coordinate the behaviors of semi-autonomous tissue units within an organ. Such coordination enables the skin to condition its responses to the spatial extent of injuries, launching a full scale regenerative response only when a sufficient threshold is reached.

RESULTS

Topology-Dependent Hair Plucking Can Induce the Regeneration of More Hairs Than Were Plucked by Activating Neighboring, Unplucked Follicles

To gain insight into the mechanisms leading to hair renewal following follicle injury, the relationship between hair plucking density and regeneration were examined in the mouse. To standardize the experiments, we synchronized all the dorsal pelage HFs into refractory telogen before plucking (see Extended Experimental Procedures). Normal hair density in adult C57BL/6 mouse dorsal skin is ~45–60 hairs/mm^2, corresponding to a distance between each follicle of ~0.15 mm (Figure S1E). In the first set of experiments, 200 evenly distributed refractory telogen hairs were plucked within a circular skin area (the "injury field"; Figures 1B and 1C, red circle). By plucking a constant number of hairs but altering the size of the injury field (Figures 1A, 1B, and S1), plucking densities from 2–50 hairs/mm^2 were obtained (Figures 1 and S1; Extended Experimental Procedures). We then studied the regenerative behavior of the HFs.

We observe three types of responses (Figure 1F). First, if 200 hairs were plucked in a large area (>6 mm diameter, 28.3 mm^2, plucking density <10 hairs/mm^2) (Figures 1B and S1), no regeneration of plucked or unplucked follicles occurs even after 30 days (Figures 1A, 1B, and S1). This is because the plucking density is too low and does not generate accumulated signals above the threshold level (Figure 1F, zone of very low density plucking, gray area). Second, when 200 hairs are plucked from 3-, 4-, or 5-mm diameter circular areas (plucking density >10 hairs/mm^2, the threshold density), we induce a simultaneous regeneration of the whole region (including the plucked and surrounding unplucked follicles) (Figures 1C and 1D). Thus, by plucking only 200 hairs, the eventual regeneration of approximately 450, 780, or 1,300 hairs are obtained (with 200 hairs plucked in injury field sizes of 3, 4, and 5 mm in diameter, or 7.1, 12.6, and 19.6 mm^2, respectively) (Figures 1C–1F, S1, and S2). As an example, we can induce regeneration of up to 600 unplucked hairs within a 5-mm plucked region (zone of quorum sensing-dependent hair regeneration, orange/light green area in Figure 1F) and 400 hairs outside of the plucked region, resulting from propagation. Third, when 200 hairs are plucked from a 2.4-mm diameter region (high density, 100% plucking), every follicle in the field is plucked (Figure 1A). In this case, all follicles re-entered anagen ~12 days (12.3 ± 3.37, n = 13) after plucking, and the number of regenerating follicles equals the number of plucked follicles (zone of all follicles plucked, dark green). Plucking-dependent regeneration from refractory telogen requires the plucking of at least 50 follicles to reach the basal threshold (Plikus et al., 2008). This zone is equivalent to the frequently used wax stripping procedure (Müller-Röver et al., 2001) in which melted wax was used to strip away all follicles in a large region, usually centimeters in diameter or bigger. This method involves thousands of HFs which will regenerate in synchrony without using quorum sensing.

The Hair Follicle Population as a Quorum-Sensing System

The density-dependence of regeneration, together with the simultaneous regeneration of both plucked and unplucked follicles within the injury field, suggests that plucked follicles produce a signal that (1) spreads to neighboring follicles, (2) accumulates to a level that depends upon the density and position of other plucked follicles, and (3) when present above some threshold level will trigger any follicle—plucked or unplucked—to re-enter anagen.

The idea that HFs produce signals that affect other HFs can be inferred from the coordinated waves of hair cycling that travel across the skin of mice and rabbits (Plikus et al., 2008, 2011). Yet the signals that coordinate such "hair waves" cannot explain the collective regenerative responses seen here, at least not those within the injury field itself. This is because hair waves reflect the ability of follicles in anagen to accelerate the progression of neighboring telogen follicles into anagen, whereas plucking causes injured and uninjured follicles to progress from refractory telogen to regenerate collectively and simultaneously (i.e., regeneration is not driven by neighboring anagen follicles). Just outside the plucked injury fields (e.g., Figure 1C, outside of the red circle), however, the ring of delayed regeneration likely reflects the "hair wave" phenomenon, since follicles in this zone enter anagen only after regeneration in neighboring follicles is well underway. To avoid confusion between initial, collective regeneration and later hair wave spreading, the present study focuses exclusively on early regenerative events.

One way to gain insight into the nature of the quorum signal—that we shall initially call the "distressor"—that coordinates collective regeneration is to characterize its decay length, i.e., the characteristic spatial scale over which the strength of the signal decays. Decay lengths quantify the balance between the rate at which a signal spreads and the rate at which it is destroyed or

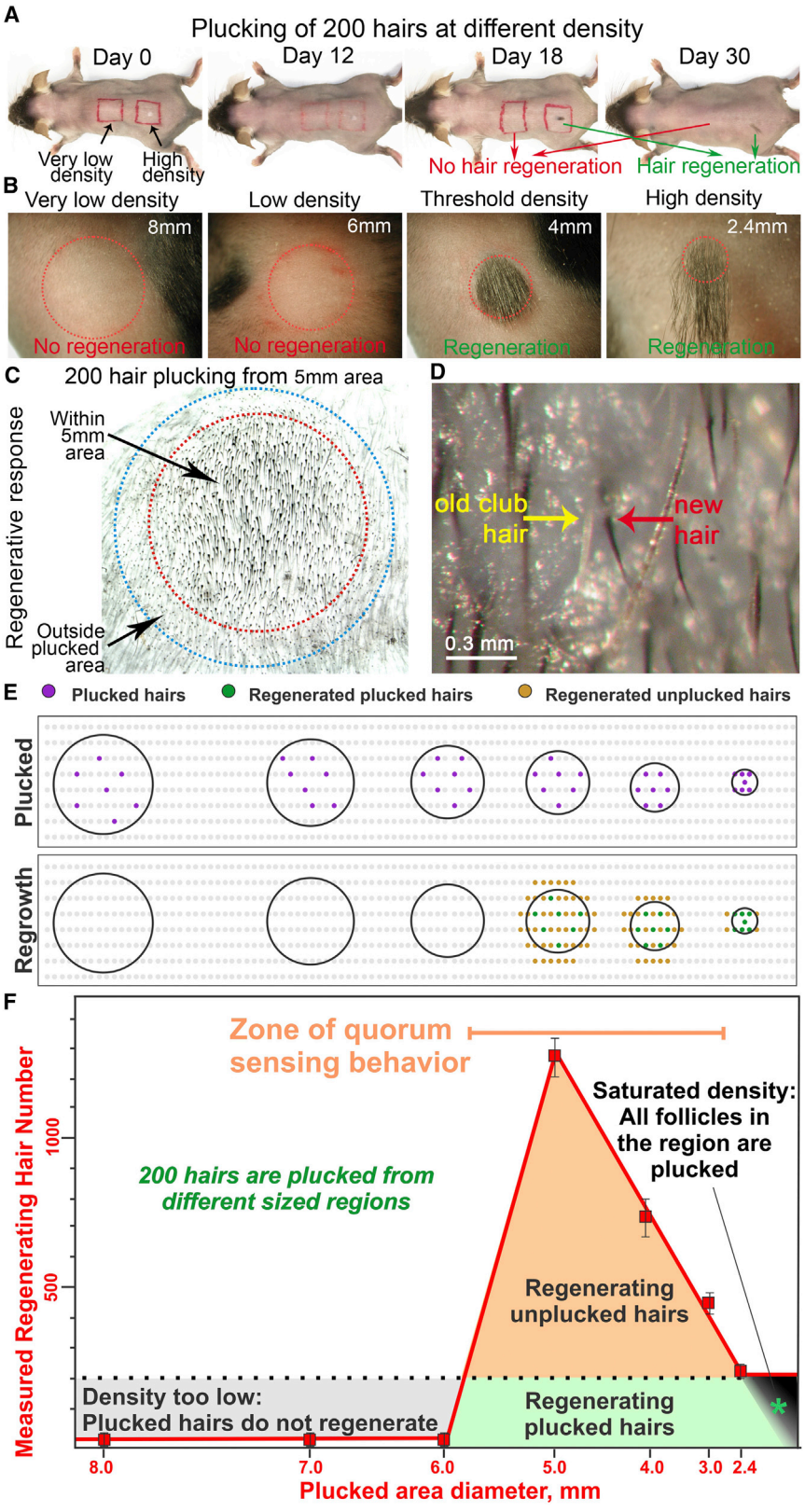

Figure 1. Plucking-Induced Hair Regeneration Is a Population-Based Behavior that Depends on the Density and Distribution of Plucked-Hair Follicles within the Unplucked Follicle Population

(A and B) Plucking 200 hairs from a circular 2.4 mm in diameter area (100% plucking) leads to hair regeneration 12 days later. Plucking 200 hairs in a 12 mm diameter area (100 mm^2 area; low density plucking) fails to induce follicle regeneration even 30 days later.

(C) Plucking induces regeneration of all follicles (the 200 plucked and 600 unplucked) within the plucked area (red circle, 5 mm in diameter). Unplucked follicles (400 HFs in total) outside the plucked area boundary then regenerate due to hair wave propagation (blue circle).

(D) High power view showing unplucked follicle regeneration: the old gray club hair (yellow) is pushed out by the regenerating black anagen hair (red).

(E) In this schematic drawing, gray dots represent telogen HFs. Black lines encircle exemplary plucked regions. Plucked follicles (purple dots). Regenerating plucked HFs (green dots). Regenerating unplucked HFs (tan dots).

(F) Plot showing the hair regeneration response versus the size of the plucked field. For all different field sizes, 200 hairs are plucked evenly dispersed throughout the field. A regenerative response is observed when 200 hairs are plucked at a density above a threshold (10 hairs/mm^2), which corresponds to plucking 200 hairs from a 5-mm diameter circular surface area (red line). Three responses represented by different colors (gray, tan, green), are observed (please see text for explanation). The quorum sensing zone is highlighted in orange.

See also Figures S1 and S2.

removed. Diffusible molecules that are captured by high-affinity, cell surface receptors (e.g., morphogens, growth factors, cytokines, and chemokines) tend to have relatively short decay lengths, typically on the order of no more than 100 μm (Teleman and Cohen, 2000; Müller et al., 2012; Sarris et al., 2012; Weber et al., 2013; Shimozono et al., 2013), approximately the same scale as the inter-follicular distance in mouse skin. In contrast, as we show in the next section, the decay length of the putative distressor induced by plucking appears to be substantially larger—on the order of 1 mm, or four to six inter-follicular distances.

Estimating the Range of Action of the Quorum Signal

Regardless of the physical nature of a signal (i.e., if it spreads from cell to cell via an undirected random walk), its spread can usually be modeled as a diffusion process, and it will display a decay length, λ, equal to the square root of the ratio between its diffusivity (an intrinsic measure of how fast it moves) and the rate constant that characterizes its removal or destruction in the tissue through which it spreads (Lander, 2007) (a physical interpretation of λ is the distance over which the steady-state signal from a point source falls by a factor of 1-1/*e*, or ~63%).

The results of modeling plucked hairs as an array of point sources of a diffusible distressor in a 2D medium (Figure 2A; see also Extended Experimental Procedures) tell us that the expected steady-state distressor concentration should be a function not only of plucking density, but also of injury field size, shape, and λ. For example, with a constant plucking density, concentrations of distressor should rise as a function of field size/λ, leveling off as that ratio gets large (Figure 2A). Assuming that regeneration is triggered when the distressor concentration around an HF exceeds a certain threshold, these results suggest that one could estimate the value of λ from a series of experiments in which plucking density and injury size/shape are both varied.

For example, in Figure 2B, data on whether regeneration in circular injury fields occurred (green dots) or failed (red dots) was tabulated as a function of field radius and plucking density (plotted, in this case, as the inverse of the plucked fraction). Fitting the boundary between positive and negative data to the predictions of the steady-state diffusion model yields estimates of λ between 0.6 and 1.6 mm (Extended Experimental Procedures).

The same model also predicts that, for sufficiently large plucked fields and/or sufficiently high plucking densities, immediate regenerative responses should not be limited to the precise boundaries of the injury field, but should extend a small distance beyond those boundaries (here we refer only to regeneration that occurs at the same time as that within the injury field and not what is triggered significantly later by hair wave propagation). Careful examination of experimental data showed that a small rim of early regeneration indeed occurred just outside of some injury fields. Fitting the sizes of these rims to the model (Figure 2C) yields an independent estimate for λ = 1 mm.

Finally, the same diffusion model suggests that λ can also be estimated by holding both plucking density and injury field area constant, but varying the shape of the injury field. To test this prediction, experiments were carried out in which 50 hairs were plucked evenly at a density of every other hair, either in a straight line (Figure 2D), a narrow rectangle (6:1 aspect ratio; Figure 2E) or a square (Figure 2F). Under these distinct topological conditions, plucked single rows never regenerated, while squares always regenerated robustly. Rectangles occasionally exhibited modest regeneration, suggesting a distressor concentration very close to threshold under these circumstances. Fitting these three behaviors requires a value of λ between 0.7 and 1.2 mm.

The good agreement among these three methods supports the validity of the steady-state diffusion model for describing distressor spreading and places the value of λ at ~1 mm. Fitting to the model does not imply, however, that the distressor is a single substance, or even a diffusible molecule, but simply that it spreads according to the same rules. In fact, the observed magnitude of λ suggests that the distressor is not simply a diffusible receptor-binding molecule, since these typically display decay lengths of one tenth this magnitude or less (Teleman and Cohen, 2000; Müller et al., 2012; Sarris et al., 2012; Weber et al., 2013; Shimozono et al., 2013). As described below, further investigation of the molecular nature of the distressor signal supports the idea that it consists of both diffusible molecules and recruited cells that migrate actively between follicles.

Plucking Induces a Cascade of Inflammatory, Cellular, and Molecular Events

Results from wax-stripping experiments indicate that HF keratinocytes undergo apoptosis ~4 hr after injury (Ito et al., 2002; see also Figure 3A). To identify molecules and mechanisms that might be involved in plucking-induced regeneration, we carried out microarray analysis of plucked fields at 12, 24, 48, and 96 hr after injury. Among the notable, time-dependent changes in gene expression, we observed:

(1) Transient increase in expression of pro-inflammatory cytokines. Immune, inflammatory and wound healing response genes constitute the major portion of early transcriptional activity following plucking. Analyzing the most altered genes by RT-PCR, we found that immune cytokines, *chemokine (C-C motif) ligand 2* (*CCL2*), *chemokine (C-X-C motif) ligand* 2 (*CXCL2*), and *interleukin 1*, *beta* (*IL-1β*) were upregulated soon after plucking (i.e., 12 hr), although expression of these genes peaked at different times (Figure 3B). For example, *CCL2* expression peaked around 12 hr (Figure 3B).

(2) Reduced refractory telogen inhibitor expression. During refractory telogen, the extra-follicular macro-environment expresses high levels of inhibitors, including *Bmp2*, *Dickkopf* (*Dkk1*), and *soluble frizzled related protein* (*Sfrp4*) that block anagen re-entry and hair wave propagation (Plikus et al., 2008, 2011). Expression of *Sfrp4*, a representative gene, decreased markedly at day 1 but rebounded by days 2 and 4 (Figure 3B).

(3) Increased tumor necrosis factor alpha (*Tnf-α*) expression. *Tnf-α* increases between 1–2 days after plucking and reached a plateau at ~day 2 (Figures 3B and 3C). The plateau of *Tnf-α* expression corresponds to a time when activated hairs are in early anagen phase (Figure 3C). We also observe changes of other molecular pathways. For example, *platelet derived growth factor A* (*Pdgf-α*) increased at later stages after plucking (day 4), compatible with published results (Festa et al., 2011) (Figure 3B).

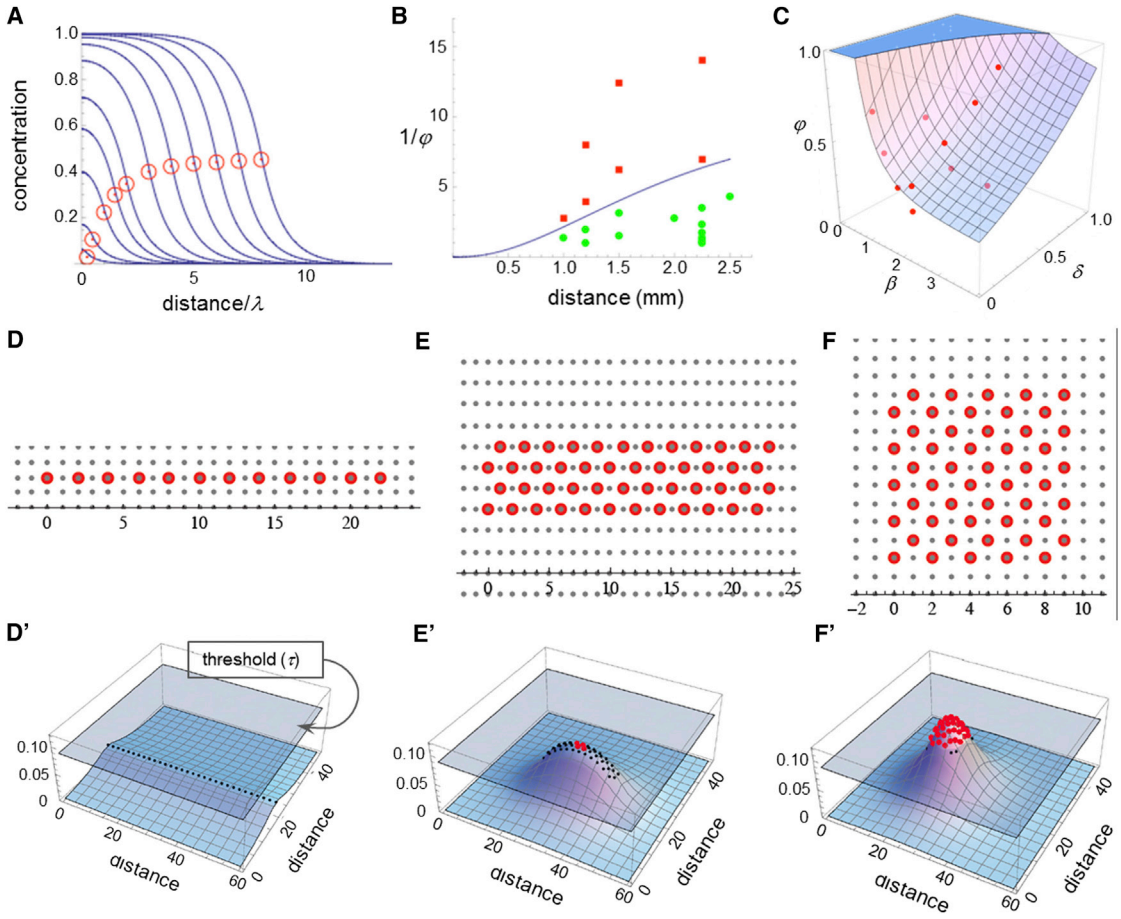

Figure 2. Mathematical Modeling Identifies the Decay Length of a Putative Quorum Signal

(A) Calculated steady-state concentrations for a diffusible substance produced within injury fields in proportion to the numbers of plucked HF. Each curve represents a different sized circular injury field, with the red circle placed at the value on the abscissa corresponding to the injury field radius, in units of the diffusing substance decay length. Specifically, the 11 curves represent increasing field sizes of 0.25, 0.5, 1, 1.5, 2, 3, 4, 5, 6, 7, and 8 decay lengths. As plucked regions grow larger, the value at the boundary asymptotes to one half the value at the center. λ is a decay length. Please see Results and Supplemental Information for more explanation.

(B) Data from a variety of regeneration experiments involving circular wound fields are plotted as a function of the inverse of the plucked fraction (φ) and the radius of the wound field. The curve drawn between the points corresponding to cases of successful (green) and unsuccessful (red) regeneration was obtained from the equations that produced the curves in (A), by fitting two parameters, the decay length and the threshold concentration for regeneration. The range of possible values consistent with the data was manually explored to yield a range of decay length estimates.

(C) The same model was used as in (B), but the data that were fit consisted of the distances, δ, just beyond the edges of injury fields at which initial regeneration was seen. (β, radius of the injury field; φ, the plucked fraction). The plotted surface represents a least-squares best fit to the data.

(D–F′) Effects of injury field shape. Fifty hairs were plucked evenly, at a density of every other hair, either in a straight line (D and D′), a narrow rectangle (6:1 aspect ratio; E and E′) or a square (F and F′). In (D′)–(F′), a discrete form of the equation used in (A)–(C), in which each HF is modeled as a discrete source, was used to plot the steady-state spatial distributions of a distressor released by plucked follicles (distances are plotted in units of the inter-follicular distance, ~0.15 mm). Wherever plotted surfaces extend above a regeneration concentration threshold (gray plane), red dots mark the location of each HF indicating successful regeneration. The requirement that these curves be consistent with the observed regeneration patterns in all three cases was sufficient to provide yet a third estimate of the distressor decay length. See also Supplemental Information on mathematical model.

Since the Wnt pathway is critical for hair growth (Enshell-Seijffers et al., 2010; Lowry et al., 2005), we examined the expression of Wnt pathway members, using whole mount in situ hybridization, and compared their expression patterns, over time, with those of *Tnf-α*. *Wnt6*, β-*catenin*, and *lymphocyte enhancer factor* (*Lef-1*) were upregulated within new anagen follicles at day 4, but not in the extra-follicular dermal macro-environment (Figure S3). We also localized *Tnf-α* expression to the extra-follicular dermal macro-environment (Figures 3C and S3).

CCL2 Is a Key Component of the Quorum Signal

The earliest noted signaling molecule expression change that could potentially communicate information from plucked to unplucked follicles was CCL2 (Figure 3B). Immunohistochemistry showed that CCL2 is primarily produced by HF keratinocytes

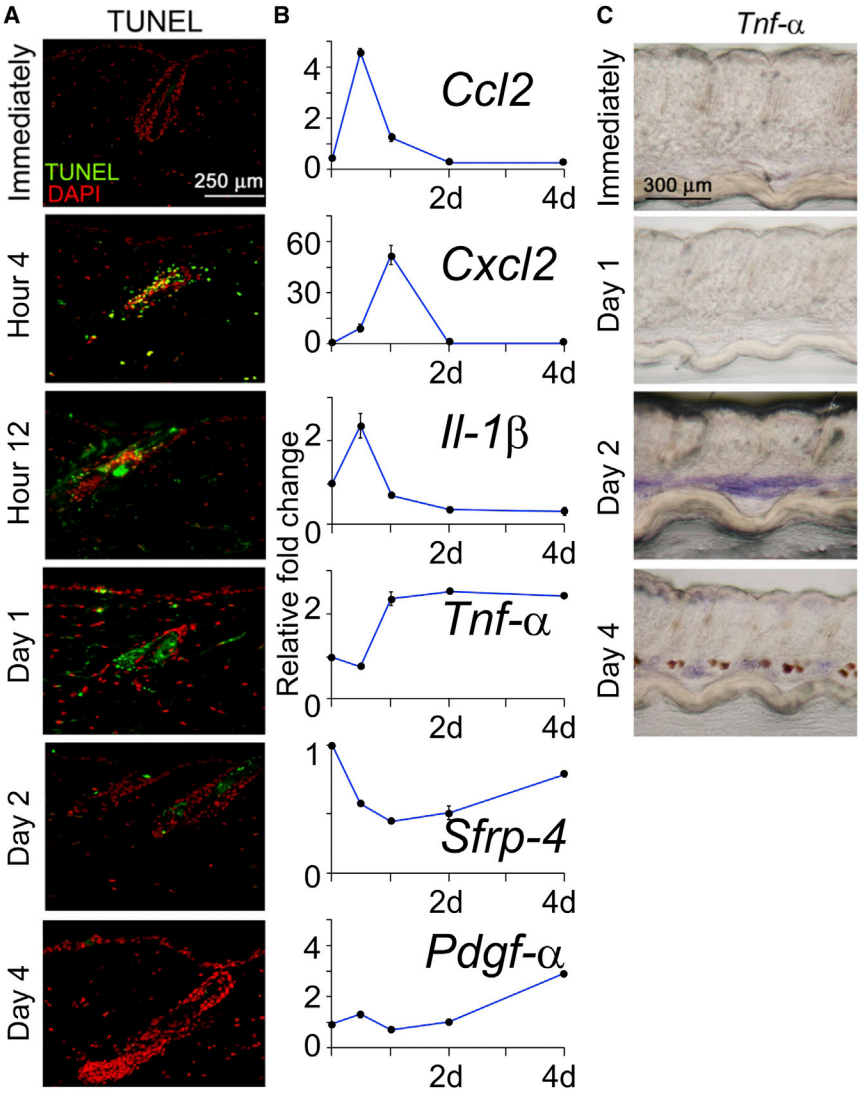

Figure 3. Identification of Macro-Environmental Modulators following Hair Plucking

(A) TUNEL assay to measure apoptosis.

(B) Real-time PCR from extra-follicular macro-environmental tissues revealed the kinetics of gene expression induced by plucking (normalized to GAPDH with 40 cycles, data are represented as mean ± SD, n = 3).

(C) Whole mount in situ hybridization showed that *Tnf-α* is markedly upregulated in the inter-follicular area beginning 2 days after wax stripping.

See also Figures S3 and S4.

and accumulates predominantly in plucked follicles (where apoptosis occurs), and to a much smaller extent in neighboring unplucked follicles, which do not undergo apoptosis (Figures 4A, 4B, and S4). This induction is transient and diminishes at day 5. CCL2 induction in plucked HFs occurred regardless of plucking density, so CCL2 was expressed even at the densities that failed to launch regeneration. Epidermal staining of CCL2 is evident in the 2.4 mm specimen, some is seen surrounding the plucked follicle in the 5 mm specimen, but staining is sparse in the 8 mm specimen.

These results are consistent with CCL2 expression providing an overall measure of the extent of plucking and therefore potentially serving as a quorum signal. To test whether CCL2 function is required for follicle regeneration, we waxed whole back skin from both wild-type C57BL/6 and CCL2 null mice. In contrast to the localized plucking of 200 hairs (that induces hair regeneration after ~12 days) (Plikus et al., 2008), wax-stripping the whole back skin drives telogen hairs back into full anagen (anagen VI) within ~6 days (Müller-Röver et al., 2001). However, when the backs of CCL2 null mice were wax-stripped, follicles remained in telogen 3 days after waxing and were still in anagen III to IV at day 6 (Figures 4C and S5A). This delayed hair regrowth in CCL2 null mice following plucking supports a role for CCL2 in plucking induced hair regeneration.

TUNEL staining performed 1 day after plucking revealed that both wild-type and CCL2 null mice showed apoptotic HF cells (Figures 4D and S5B). These results indicate that CCL2 is not required for the initial injury response of HFs, but rather its expression is triggered by that response, whereupon it plays an important role in regeneration. This view is consistent with a recent study showing that various HF regions express chemokines including CCL2, CCL20, and CCL8 in response to stress (Nagao et al., 2012a). The percent HF area with CCL2 expression was highest 1 day after plucking and decreased thereafter (Figure 4E). Unplucked follicles located within (x) or outside (y) of the plucked field showed low and no CCL2 levels. CCL2 null mice did not express CCL2 after plucking (z).

M1 Macrophages Are Mediators Recruited by CCL2 to Execute Quorum-Sensing Behavior

The decay lengths of most diffusible signaling molecules, including chemokines (Sarris et al., 2012; Weber et al., 2013), are much shorter than the decay length we measured for the plucking-induced quorum signal (Figure 2). Chemokines, however, are known to act as chemo-attractants for immune cells, and we postulated that this might play a role in boosting the effective range of action of an initial quorum signal. CCL2 in particular is a potent recruiter of monocyte/macrophage lineage cells.

Indeed, 2 days after plucking, macrophages had heavily infiltrated the plucked skin (Figure 5A). We quantified the macrophage distribution at different times after plucking (Figure 5E). At day 1, F4/80 positive macrophages accumulate around and between the plucked follicles. At day 3, more macrophages spread to the inter-plucked follicular regions and their density

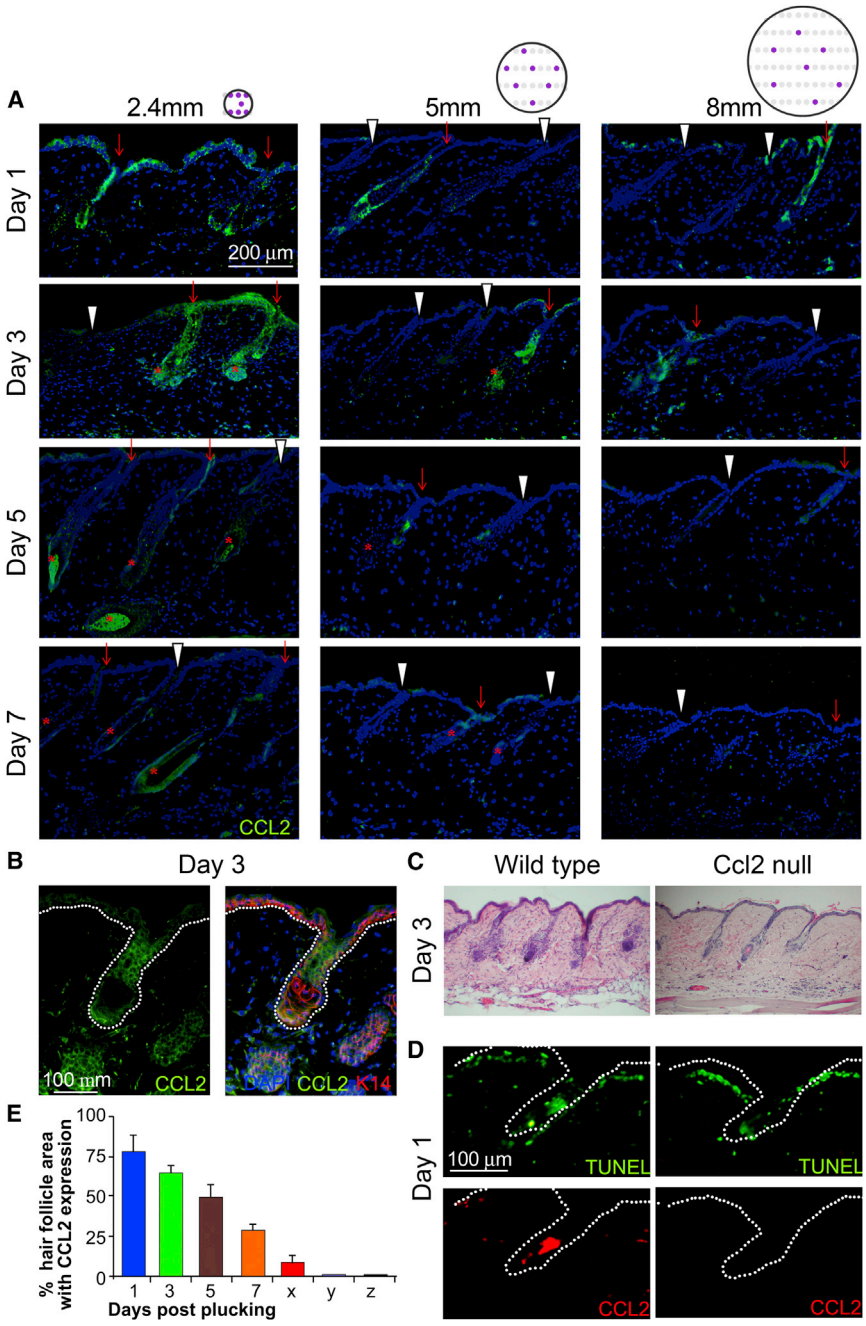

Figure 4. CCL2 Is Involved in Plucking Induced Hair Regeneration

(A) HF keratinocytes showed higher CCL2 expression (green) in plucked follicles (red arrow) than in unplucked follicles (white arrowhead). The circle with purple dots indicates the topology of plucked follicles (see also Figure 1E). Peak expression occurs 1–3 days after plucking, and no marked difference between the 2.4, 5, and 8 mm groups were noted. Asterisk represents regenerating HFs.

(B) Double immunostaining for K14 and CCL2 of samples 3 days after plucking showed that HF keratinocytes in plucked follicles are the main source of CCL2.

(C) Hair re-growth is retarded when hairs were plucked from CCL2 null mice.

(D) CCL2 null mice showed similar apoptotic HF cells following plucking as wild-type mice, but could not induce CCL2 in apoptotic HF cells.

(E) Graph showing the percentage of HF area expressing CCL2 at 1, 3, 5, and 7 days post-plucking as well as unplucked HFs within (x) and outside (y) of the plucked field. CCL2 null mice do not express CCL2 (z). (n = 3). Data are represented as mean ± SD.

See also Figure S5.

is substantially elevated (at least four times over background) up to 66% of that found for plucked follicles. The spread can span a distance of 1 mm. These macrophages start to dissipate at day 7 post-plucking.

To test whether macrophages play a functional role in plucking-induced hair regeneration, we used chemical inhibitor and genetic deletion assays. The application of Clodronate liposomes to suppress macrophage function caused an ~12-day delay in hair plucking induced regeneration (Figure 6F). For the genetic approach, we used *LysM-Cre;R26R* transgenic mice to examine the distribution of LacZ positive myeloid cells following hair plucking. Myeloid cells are nearly absent in normal mice, but are induced at days 3–5 and diminish at day 7 in the transgenic mice (Figure 5F).

To evaluate their role, we generated a triple transgenic mouse model where myeloid cells are specifically depleted by diphtheria toxin upon doxycycline treatment (*LysM-Cre;Rosa-rtTA;TetO-DTA*). We plucked 200 hairs/5 mm diameter region, which usually launches a quorum sensing response, leading to regeneration. In this mutant, hair regeneration did not occur (Figures 5G and S2D). These myeloid cells represent mainly macrophages, although technically we cannot rule out other cell types completely. All together, the data suggest macrophages play a major role in this process.

Macrophages can be divided into two major types; M1 macrophages (classically activated) exert proinflammatory activities, and M2 macrophages (alternatively activated) are involved in resolving inflammation (Gordon, 2003; Willenborg et al., 2012). Immunostaining showed that M1, but not M2 macrophages, were present 5 days post-plucking (Figures 5B, 5C, and S6A).

These findings are consistent with other studies implicating chemokines in the recruitment of inflammatory macrophages during wound healing and a role for such cells in tissue repair (Willenborg et al., 2012). Since M1 macrophages express CCR4 (Figures 5D and S6A), the receptor for CCL2, we think that these macrophages are recruited to plucked

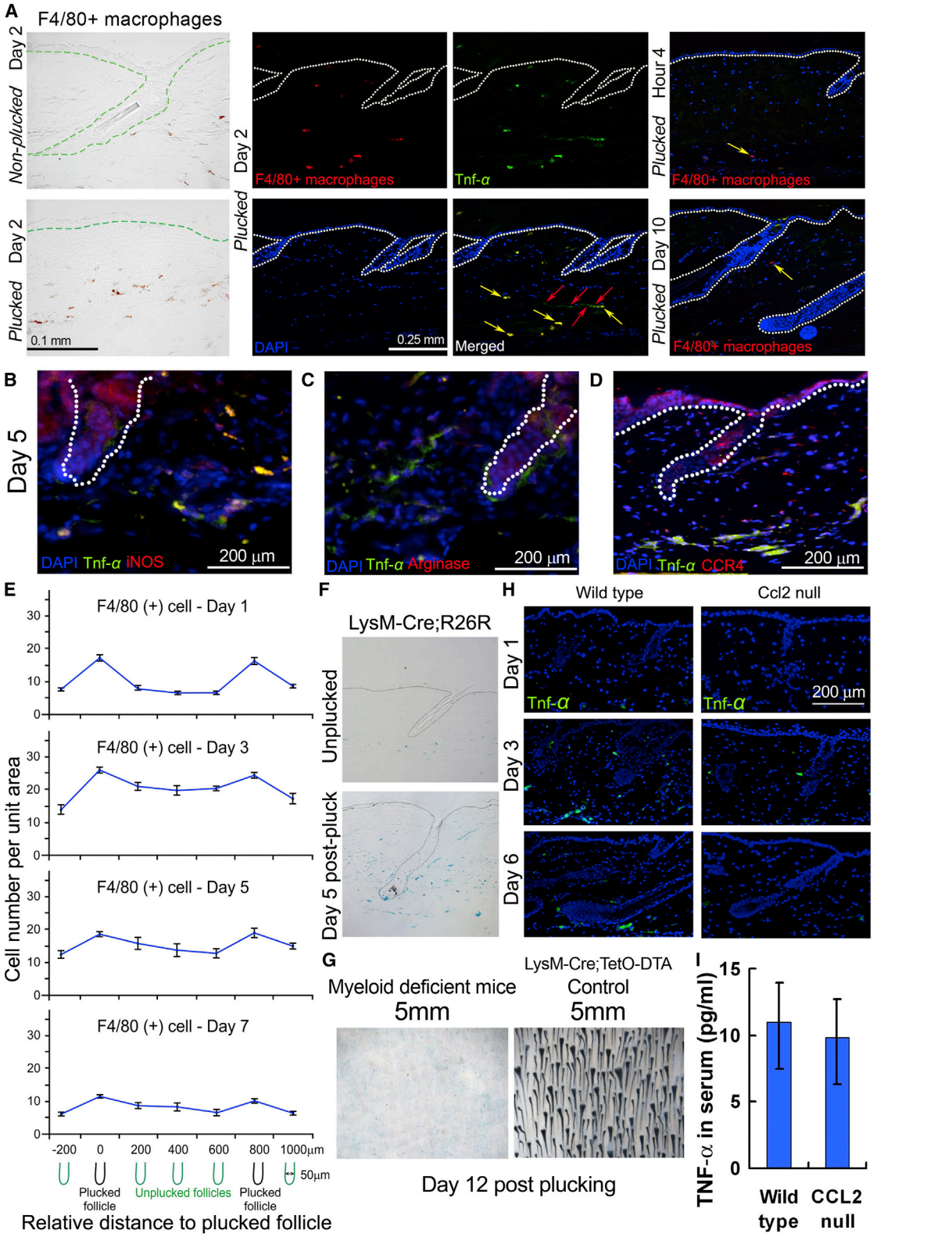

(legend on next page)

follicles by plucking-induced CCL2. Consistent with this view, plucking failed to induce the accumulation of M1 macrophages in CCL2 null mouse skin (Figure 5H). These data support the model that CCL2 expressed by plucked follicles recruits CCR4-expressing M1 macrophages, which play an essential role in regeneration. We next explored how this comes about.

Hair Regeneration Induced by Quorum Sensing Is Tnf-α Dependent

Macrophages are known to produce Tnf-α. *Tnf-α* mRNA was induced ~2 days after plucking, before anagen initiates (Figures 3B, 3C, and S3). Low power whole mount in situ hybridization reveals that, under conditions in which regeneration occurs, Tnf-α is enriched in the extra-follicular environment of both plucked and unplucked hairs (Figure 6A). Double immunostaining showed that these cells are indeed M1 macrophages (Figures 5B, 5C, 5D, 6B, and S6).

Semiquantitative analysis of immunostained specimens obtained from regions of different plucking densities support the view that Tnf-α expressing macrophages accumulate around HFs that regenerate after plucking (both plucked and unplucked), but do not accumulate under plucking conditions that fail to activate hair regeneration (Figure S6D).

Quantitative measurements of macrophage-derived Tnf-α immunoreactivity over time in a threshold-plucking density region (200 hairs/5 mm diameter) showed that Tnf-α positive cells are induced around plucked follicles. They then increased significantly at day 3 and 5 after plucking, spreading into the dermal region between plucked follicles. They decreased at day 7 to approach basal levels (Figures 5E, 6C, and S7B).

To investigate the functional importance of Tnf-α in plucking-induced hair regeneration, beads coated with Tnf-α-related peptide were injected into refractory telogen stage mouse skin. Hair regeneration was induced, followed by propagation to the surrounding region (Figure 6E). Control bead injection did not induce hair regeneration even after 30 days (Figure 6G). Conversely, when hairs were plucked at high density in Tnf-α null mice (Figure 6F), a 15-day delay in regeneration was observed. These results indicate that Tnf-α is one of the major players for plucking-induced hair regeneration.

Last, we searched for molecules and signals that might function further downstream in hair regeneration. For example, Tnf-α is known to stimulate both JNK and NF-κB (nuclear factor kappa-light-chain-enhancer of activated B cell) signaling. It is also known that activation of the FGF signaling pathway can trigger hair regeneration (Greco et al., 2009). We therefore screened inhibitors of NF-κB, JNK, PI3K, FGF receptor, p38 MAPK, and Erk for effects on plucking-induced hair regeneration. Only NF-κB inhibitors delayed hair regeneration, doing so by 10 days (Figures 6H and S7C). In addition, Tnf-α-related peptide significantly stimulates the expression of Wnt3, Wnt10a, and Wnt10b in keratinocytes (Figure 6I). Although the Eda-NF-κB pathway is important in hair development, a previous study indicated that Eda participates in anagen to catagen transition during the postnatal hair regeneration cycle (Fessing et al., 2006). Hence, it is not likely that Eda is involved in the plucking induced hair regeneration response. Together the results raise the possibility that Tnf-α, acting through the NF-κB pathway, ultimately stimulates hair regeneration through activation of Wnt signaling.

DISCUSSION

Social Behaviors in an Organ Population

Many organs are composed of repeated, semi-autonomous tissue units, such as acini, crypts, and follicles. The potential for dynamic coupling between the behaviors of such units creates opportunities for collective phenomena. A dramatic example of this is the "hair wave," a coordinated hair cycle wave that can travel across the skin of mammals (Suzuki et al., 2003; Plikus et al., 2008, 2011; Murray et al., 2012).

In this work, we characterize another collective behavior of HFs; density- and topology-dependent, plucking-induced regeneration, which can be viewed as a form of quorum sensing. Quorum sensing is a process whereby a population makes a collective decision based on the number or density of individuals that meet a certain criterion. Typically, a response occurs only when a threshold is exceeded. Quorum sensing has been invoked to describe bacterial cell-to-cell communication (Bassler, 2002) that serves to influence gene regulation in response to population density fluctuations (Miller and Bassler, 2001). Synthetic quorum sensing circuits in yeast were used to demonstrate the diversity of social behaviors that can come from collective communication (Youk and Lim, 2014). Quorum sensing also has been used to explain the collective decision-making behavior of social insects such as ants and honey bees (Pratt, 2005; Visscher, 2007).

Figure 5. CCL2 Stimulates Tnf-α Production by Attracting CCR4 (+) M1 Macrophages

(A) Tnf-α is upregulated in the dermal macro-environment on day 2 after wax stripping. Tnf-α in the dermal macro-environment is produced by both dermal macrophages (F4/80+ cells, yellow arrow) and adipose cells (red arrow; see also Figure S5C). Few macrophages (yellow arrow) are present at hour 4 and day 10 after plucking. These macrophages do not express Tnf-α.

(B and C) Staining shows that Tnf-α is mainly produced by M1 (iNOS-positive) rather than M2 (Arginase-positive) macrophages.

(D) Tnf-α (+) cells express CCR4 in response to CCL2.

(E) The number of F4/80+ cells is highest near plucked follicles and their density decreases with increasing distance from the plucked follicles. See Figure S7A for the unit area we quantified for each data point. The number of F4/80+ cells is rapidly elevated at day 1 post-plucking, reaching a maximum at day 3 and then diminishing at 5 and 7 days after plucking.

(F) *LysM-Cre;R26R* reporter mice show that the myeloid lineage-derived cells mostly are induced in the dermis around plucked HFs.

(G) When 200 hairs were plucked from myeloid cell-deficient mice from 5 mm region, hairs cannot be induced.

(H) Tnf-α (+) cells was not induced in CCL2 null mice.

(I) Tnf-α serum levels are similar between wild-type and CCL2 null mice. Data are represented as mean ± SD.

See also Figures S6 and S7.

Molecular Nature of the Quorum-Sensing Circuit

Briefly, the quorum sensing circuit we describe here provides a way for injured HFs to collectively assess the magnitude and extent of injury that the skin has sustained and make an all-or-none decision whether or not to regenerate. A striking feature of this circuit, revealed through molecular modeling, is that the information being shared among follicles decays with a characteristic length of ~1 mm, substantially greater than the measured decay lengths of diffusible signaling molecules (Teleman and Cohen, 2000; Müller et al., 2012; Sarris et al., 2012; Weber et al., 2013; Shimozono et al., 2013). The explanation for this apparent paradox seems to reside in the multi-stage nature of the quorum signal, which begins with diffusible molecules, but eventually involves the recruitment of motile cells (inflammatory macrophages) that spread within the tissue. Below we summarize the sequence of molecular and cellular events revealed by the present study (Figure 7).

(1) Micro-injury and inflammation. Hair plucking leads to hair keratinocyte apoptosis (Ito et al., 2002) (Figure 3A). This in turn leads to inflammatory changes and to the localized overexpression of several inflammatory cytokines, especially CCL2, which may be detected within 12 hr post-plucking (Figures 3B and 4).

(2) Molecular signal release and dissemination. CCL2 and other cytokines are secreted from plucked follicles and may also involve epidermis around the plucked follicle. The importance of CCL2 is demonstrated by the fact that, in CCL2 null skin, regeneration is markedly delayed (Figure 4). The fact that it is not prevented entirely suggests that some other cytokines induced by plucking may act redundantly with CCL2.

(3) Recruitment of macrophages as motile vectors. The local production of CCL2 appears to recruit CCR4 (+) M1 macrophages in the dermis (Figure 5). Whereas macrophages initially appear to be enriched around plucked follicles, recruited macrophages soon spread throughout the whole region. By relaying a signaling response with a motile cellular vector, HFs effectively solve the problem of spreading quorum information over long distances.

Another motile vector candidate is the epidermal dendritic Langerhans cell since it also expresses F4/80 antigen. However, F4/80 positive cells appear in dermis at day 1, but do not appear in the epidermis until days 5–7. Our microarray data also did not reveal upregulation of Langerhans cell markers, such as CD207 (Langerin) and CD11b. Although we do not completely rule out the involvement of Langerhans in this process, our data so far suggest a major role for dermal macrophages in this process.

It is worthwhile to mention here that more examples of extended cellular process that mediate signal communication are being identified. For example, in zebrafish stripe pattern formation, pigment cells can utilize their contact-dependent depolarization and repulsive behavior as non-diffusible inhibitors that follow Turing principles (Inaba et al., 2012). In *Drosophila* epithelia, cytonemes can establish a dynamic hedgehog morphogen gradient that may reach afar (Bischoff et al., 2013). Future in vivo imaging studies of the mouse skin model studied here will allow us to elucidate the interactive cellular behaviors between HFs, immune system and regeneration.

(4) Release of Tnf-α and collective regeneration. Inflammatory macrophages that are recruited to wound fields secrete Tnf-α, which has been shown to activate hair cycle regeneration (Figure 6E) (Duheron et al., 2011). Regeneration is greatly impaired in Tnf-α null mice (Figure 6F); moreover, Tnf-α serum levels are normal in CCL2 null mice that show impaired plucking-induced regeneration (Figure 5I). These studies indicate that local, not systemic Tnf-α is required for regeneration. Although the exact mechanism by which Tnf-α triggers follicle regeneration is not clear, the data suggest that Tnf-α may act through NF-κB which in turn activate canonical WNT signaling (Figure 6D) (Cawthorn et al., 2007; Schwitalla et al., 2013). While Tnf-α immunoreactivity is mainly in macrophages, it is also detected in other cell types and may provide additional possible mechanisms. The EDAR pathway may also activate NF-κB. However, EDAR it is more involved in anagen/catagen transition (Fessing et al., 2006), not telogen/anagen transition. Further, it is not induced in our microarray data (not shown).

Adaptive Role of Quorum Sensing

Depending on the severity of skin injury, the body may use different mechanisms to alert, defend, and regenerate the damaged tissue. Plucking of a single hair follicle is a micro-injury. An open, full-thickness wound is a catastrophic event (i.e., macro-injury). While wounded skin is known to induce hair regeneration, small and large wounds may share a fundamental mechanism, but use different molecular circuits to achieve different levels of restoration and regeneration. Indeed, HF activities have been linked to the wound-healing and regenerative behaviors of the inter-follicular epidermis. This link may be mediated by the immune system (Paus et al., 1998), macrophage recruitment (Osaka et al., 2007), and increased Tnf-α expression (Jiang et al., 2010). Interestingly, TNF-α converting enzyme, a regulator of Tnf-α, is a component of the HF bulge niche (Nagao et al., 2012b). Anagen phase HFs can influence the surrounding epidermis to markedly accelerate wound healing (Ansell et al., 2011). In mice, loss of full thickness skin larger than 1 cm in diameter could lead to new follicle formation (Ito et al., 2007). However, plucking does not launch a full wound healing response, so conceptually plucking works differently from the wound and our study focuses at a different scale. It provides a novel understanding into how HFs respond to injury at the level of a HF population. We analyzed how interactions among HFs and the dermal environment reach a binary choice based on a collective measurement of injury. We show that effective damage control is achieved via co-option of existing signaling mechanisms (e.g., Tnf-α, macrophage) for the "social behaviors" of a stem cell population.

In summary, we report a higher level integration of signals from hair regeneration, immune cytokines, and wound healing. Instead of a top-down process, quorum sensing represents a bottom-up process based on local information. Each follicle

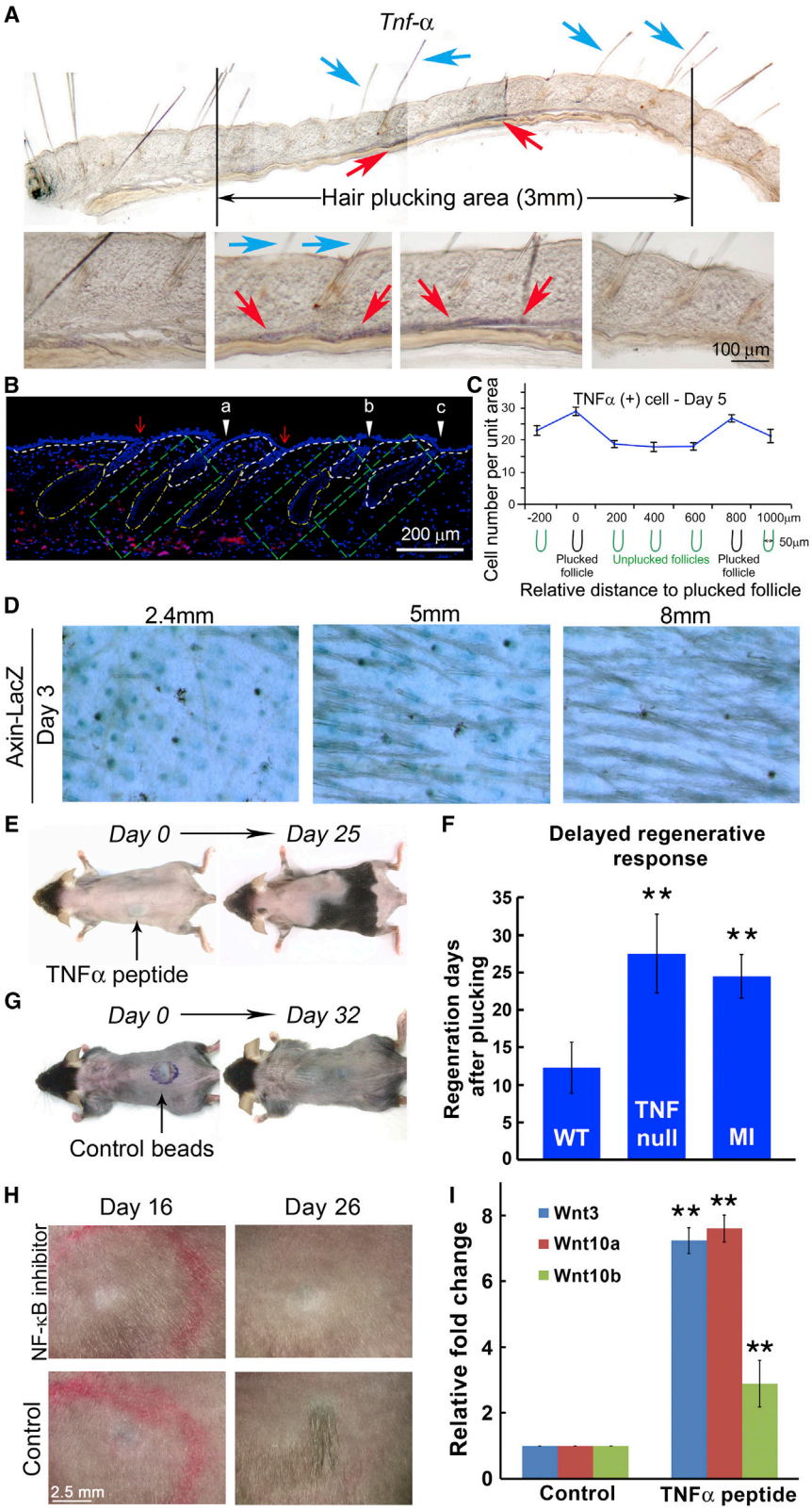

Figure 6. Hair Regeneration Is Proportional to the Local Concentration of Tnf-α

(A) Whole mount in situ hybridization shows Tnf-α (brown color in the dermis, red arrows) was induced under plucked and unplucked hairs (blue arrows) toward the center of the 3 mm plucked zone 5 days after plucking.

(B) Semiquantitative assessment of the Tnf-α concentration using the 5mm group at day 5. Its expression level was quantified in three different skin regions (green boxes) that differ in their proximity to plucked follicles. "a" is closest to the plucked follicles and shows the highest Tnf-α levels. "b" is away from the plucked follicles and shows lower Tnf-α levels. "c" is furthest away and shows the least Tnf-α.

(C) Quantitative assessment of the Tnf-α positive cells around plucked follicles and inter-plucked follicle dermis. See Figure S7B for complete series. The pattern is similar to that of F4/80 macrophage distribution (n = 3).

(D) Density-dependent plucking on *Axin-LacZ* mice show that the canonical Wnt/β-catenin signaling pathway was activated 3 days after plucking and the number of LacZ (+) HFs was proportional to the plucking density.

(E) Subcutaneous injection of Tnf-α-related peptide coated beads during refractory telogen can induce anagen re-entry and then propagate to the surrounding HFs.

(F) Tnf-α null mice exhibit a 15-day delay in anagen re-entry following plucking of 200 hairs during refractory telogen phase. Intra-peritoneal macrophage inhibitor (MI) injection can also delay plucking induced hair regeneration by 12 days.

(G) Albumin coated beads injection showed no anagen re-entry even after 32 days.

(H) Subcutaneous NF-κB inhibitor injection can delay plucking-induced hair regeneration by 10 days.

(I) Wnt3, Wnt10a, and Wnt10b were activated in keratinocytes by TNF-related peptides. Data are represented as mean ± SD. **p < 0.001.

See also Figures S6 and S7.

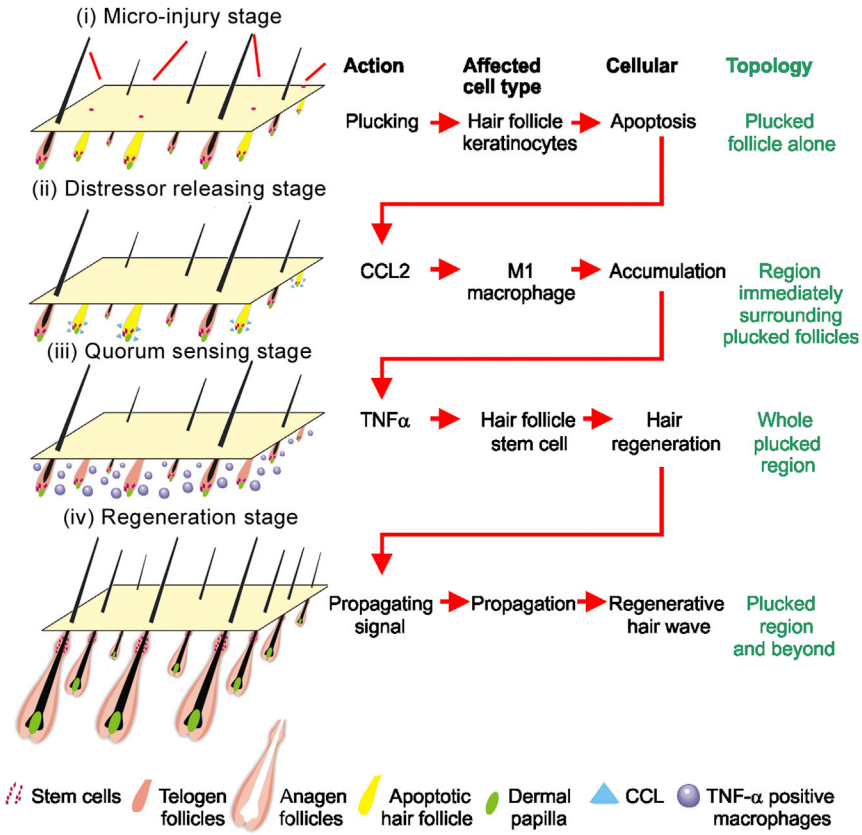

Figure 7. Molecular Basis of Quorum-Sensing Behavior during the Activation of Hair Stem Cells in the Follicle Population

Schematic illustration of the process. Stage i: minor injury → hair keratinocyte apoptosis → CCL2 production. Stage ii: CCL2 secretion → macrophage accumulation. Stage iii: macrophage and Tnf-α permeate the whole region. Stage iv: Tnf-α activates hair regeneration in the whole region. Hair regeneration further spreads due to propagation of regenerative hair waves. Please see text for more detail of the model.

becomes a sensor for the population to assess the level of damage. The molecular circuit quantifies injury strength by summing together local signals from different organs. Here, the communication among tissues reaches a larger scale organization by coupling local molecular signaling (in the form of a chemical gradient) with motile cellular vectors. In this study, macrophages are identified as a motile vector that allows a length scale of up to 1 mm. In this manner, the injury response is measured and reflects local needs. This study may just be one of the examples that reveal collective cellular behaviors in response to physiological or pathological stimuli. We believe that the quorum sensing behavior principle is likely to be present in the regeneration of tissue and organs beyond the skin.

EXPERIMENTAL PROCEDURES

Surgical Procedures

All procedures were performed on anesthetized animals with protocols approved by the University of Southern California Institutional Animal Care and Use Committee (USC IACUC). Hair cycle was synchronized by wax stripping (Müller-Röver et al., 2001). Hairs in refractory telogen were plucked with the spacing indicated in the result section. Regenerative hair numbers are counted under a dissection microscope.

RNA Preparation and Microarray

For microarray, all the dermal tissues are collected. RNA was prepared using TRI Reagent BD (Sigma-Aldrich) following the manufacturer's recommendations. Please see Extended Experimental Procedures for detail. The microarray data reported here have been submitted to the GEO (accession number GSE46181). Primer sequences for RT-PCR are listed in Table S1.

Perturbation of Quantitative Plucking

Small molecular inhibitor or peptides were injected intra-dermally on one side of mouse dorsal skin for 4 days. Then 200 hairs were plucked in the center of the injected area. After plucking, these drugs were continuously injected for an additional 6 days. DMEM was injected to the opposite side as a control. Each animal was injected with only one reagent.

ACCESSION NUMBERS

The GEO accession number for the microarray data reported in this paper is GSE46181.

SUPPLEMENTAL INFORMATION

Supplemental Information includes Extended Experimental Procedures, seven figures, and one table and can be found with this article online at http://dx.doi.org/10.1016/j.cell.2015.02.016.

AUTHOR CONTRIBUTIONS

C.C.C. and C.M.C. conceived the overall experimental design. C.C.C. and T.X.J. did the hair plucking and characterization. L.W., S.S., and M.W.H. did immune characterization. A.D.L. and P.J.M. did mathematical modeling. A.D.L. did mathematical estimation of length scale for quorum sensing. M.V.P., R.R., and C.F.G.-J. did LysM-Cre mouse work. C.C.C., C.M.C., A.D.L., M.V.P., R.B.W., and O.L. did manuscript writing and editing.

ACKNOWLEDGMENTS

C.M.C., T.X.J., and R.B.W. are supported by National Institute of Arthritis and Musculoskeletal and Skin Diseases (NIAMS) RO1-AR42177, AR 47364, and AR60306. C.C.C. is supported by NSC 100-2314-B-075-044, NSC 101-2314-B-075-008-MY3, and the Taipei Veterans General Hospital (VN103-12, V103C-010, V102B-009, R-1100403). A.D.L. is supported by NIGMS P50-GM076516. S.S. is supported by NIH R01DE17449. L.W. is supported by the National Natural Science Foundation of China (81270015). M.V.P. is supported by NIAMS R01-AR067273 and Edward Mallinckrodt Jr. Foundation grant. R.R. is supported by a California Institute of Regenerative Medicine (CIRM) training grant (TG2-01152). C.F.G.-J. is supported by the National Science Foundation Graduate Research Fellowship Program (DGE-1321846). P.J.M. is supported by a post-doctoral and early career researcher exchange fellowship from the Northern Research Parternship (NRP). M.W.H. is supported by Top Notch University plan of CKU, Taiwan. We thank Drs. Jaw-Ching Wu, Han-Nan Liu, and Yun-Ting Chang of National Yang Ming University/Taipei Veterans General hospital for their support. Invention number 2014-255 "Enhance hair growth via plucking" (D2014-0054) was disclosed to University of Southern California.

Received: May 22, 2014
Revised: January 12, 2015
Accepted: February 2, 2015
Published: April 9, 2015

REFERENCES

Ansell, D.M., Kloepper, J.E., Thomason, H.A., Paus, R., and Hardman, M.J. (2011). Exploring the "hair growth-wound healing connection": anagen phase promotes wound re-epithelialization. J. Invest. Dermatol. *131*, 518–528.

Bassler, B.L. (2002). Small talk. Cell-to-cell communication in bacteria. Cell *109*, 421–424.

Bischoff, M., Gradilla, A.C., Seijo, I., Andrés, G., Rodríguez-Navas, C., González-Méndez, L., and Guerrero, I. (2013). Cytonemes are required for the establishment of a normal Hedgehog morphogen gradient in Drosophila epithelia. Nat. Cell Biol. *15*, 1269–1281.

Cawthorn, W.P., Heyd, F., Hegyi, K., and Sethi, J.K. (2007). Tumour necrosis factor-α inhibits adipogenesis via a beta-catenin/TCF4(TCF7L2)-dependent pathway. Cell Death Differ. *14*, 1361–1373.

Chen, C.C., and Chuong, C.M. (2012). Multi-layered environmental regulation on the homeostasis of stem cells: the saga of hair growth and alopecia. J. Dermatol. Sci. *66*, 3–11.

Chuong, C.M., Randall, V.A., Widelitz, R.B., Wu, P., and Jiang, T.X. (2012). Physiological regeneration of skin appendages and implications for regenerative medicine. Physiology (Bethesda) *27*, 61–72.

Collins, H.H. (1918). Studies of normal moult and of artificially induced regeneration of pelage in Peromyscus. J. Exp. Zool. *27*, 73–99.

Duheron, V., Hess, E., Duval, M., Decossas, M., Castaneda, B., Klöpper, J.E., Amoasii, L., Barbaroux, J.B., Williams, I.R., Yagita, H., et al. (2011). Receptor activator of NF-kappaB (RANK) stimulates the proliferation of epithelial cells of the epidermo-pilosebaceous unit. Proc. Natl. Acad. Sci. USA *108*, 5342–5347.

Enshell-Seijffers, D., Lindon, C., Kashiwagi, M., and Morgan, B.A. (2010). beta-catenin activity in the dermal papilla regulates morphogenesis and regeneration of hair. Dev. Cell *18*, 633–642.

Fessing, M.Y., Sharova, T.Y., Sharov, A.A., Atoyan, R., and Botchkarev, V.A. (2006). Involvement of the Edar signaling in the control of hair follicle involution (catagen). Am. J. Pathol. *169*, 2075–2084.

Festa, E., Fretz, J., Berry, R., Schmidt, B., Rodeheffer, M., Horowitz, M., and Horsley, V. (2011). Adipocyte lineage cells contribute to the skin stem cell niche to drive hair cycling. Cell *146*, 761–771.

Gordon, S. (2003). Alternative activation of macrophages. Nat. Rev. Immunol. *3*, 23–35.

Greco, V., Chen, T., Rendl, M., Schober, M., Pasolli, H.A., Stokes, N., Dela Cruz-Racelis, J., and Fuchs, E. (2009). A two-step mechanism for stem cell activation during hair regeneration. Cell Stem Cell *4*, 155–169.

Inaba, M., Yamanaka, H., and Kondo, S. (2012). Pigment pattern formation by contact-dependent depolarization. Science *335*, 677.

Ito, M., Kizawa, K., Toyoda, M., and Morohashi, M. (2002). Label-retaining cells in the bulge region are directed to cell death after plucking, followed by healing from the surviving hair germ. J. Invest. Dermatol. *119*, 1310–1316.

Ito, M., Yang, Z., Andl, T., Cui, C., Kim, N., Millar, S.E., and Cotsarelis, G. (2007). Wnt-dependent de novo hair follicle regeneration in adult mouse skin after wounding. Nature *447*, 316–320.

Jahoda, C.A., and Christiano, A.M. (2011). Niche crosstalk: intercellular signals at the hair follicle. Cell *146*, 678–681.

Jiang, S., Zhao, L., Teklemariam, T., and Hantash, B.M. (2010). Small cutaneous wounds induce telogen to anagen transition of murine hair follicle stem cells. J. Dermatol. Sci. *60*, 143–150.

Lander, A.D. (2007). Morpheus unbound: reimagining the morphogen gradient. Cell *128*, 245–256.

Lowry, W.E., Blanpain, C., Nowak, J.A., Guasch, G., Lewis, L., and Fuchs, E. (2005). Defining the impact of beta-catenin/Tcf transactivation on epithelial stem cells. Genes Dev. *19*, 1596–1611.

Miller, M.B., and Bassler, B.L. (2001). Quorum sensing in bacteria. Annu. Rev. Microbiol. *55*, 165–199.

Müller, P., Rogers, K.W., Jordan, B.M., Lee, J.S., Robson, D., Ramanathan, S., and Schier, A.F. (2012). Differential diffusivity of Nodal and Lefty underlies a reaction-diffusion patterning system. Science *336*, 721–724.

Müller-Röver, S., Handjiski, B., van der Veen, C., Eichmüller, S., Foitzik, K., McKay, I.A., Stenn, K.S., and Paus, R. (2001). A comprehensive guide for the accurate classification of murine hair follicles in distinct hair cycle stages. J. Invest. Dermatol. *117*, 3–15.

Murray, P.J., Plikus, M.V., Maini, P.K., Choung, C.M., and Baker, R.E. (2012). Modelling hair follicle growth dynamics as an excitable medium. PLoS Comp. Biol. *8*, e1002804.

Nagao, K., Kobayashi, T., Moro, K., Ohyama, M., Adachi, T., Kitashima, D.Y., Ueha, S., Horiuchi, K., Tanizaki, H., Kabashima, K., et al. (2012a). Stress-induced production of chemokines by hair follicles regulates the trafficking of dendritic cells in skin. Nat. Immunol. *13*, 744–752.

Nagao, K., Kobayashi, T., Ohyama, M., Akiyama, H., Horiuchi, K., and Amagai, M. (2012b). Brief report: requirement of TACE/ADAM17 for hair follicle bulge niche establishment. Stem Cells *30*, 1781–1785.

Osaka, N., Takahashi, T., Murakami, S., Matsuzawa, A., Noguchi, T., Fujiwara, T., Aburatani, H., Moriyama, K., Takeda, K., and Ichijo, H. (2007). ASK1-dependent recruitment and activation of macrophages induce hair growth in skin wounds. J. Cell Biol. *176*, 903–909.

Paus, R., van der Veen, C., Eichmüller, S., Kopp, T., Hagen, E., Müller-Röver, S., and Hofmann, U. (1998). Generation and cyclic remodeling of the hair follicle immune system in mice. J. Invest. Dermatol. *111*, 7–18.

Plikus, M.V., Mayer, J.A., de la Cruz, D., Baker, R.E., Maini, P.K., Maxson, R., and Chuong, C.M. (2008). Cyclic dermal BMP signalling regulates stem cell activation during hair regeneration. Nature *451*, 340–344.

Plikus, M.V., Baker, R.E., Chen, C.C., Fare, C., de la Cruz, D., Andl, T., Maini, P.K., Millar, S.E., Widelitz, R., and Chuong, C.M. (2011). Self-organizing and stochastic behaviors during the regeneration of hair stem cells. Science *332*, 586–589.

Pratt, S.C. (2005). Quorum sensing by encounter rates in the ant Temnothorax albipennis. Behav. Ecol. *16*, 488–496.

Sarris, M., Masson, J.B., Maurin, D., Van der Aa, L.M., Boudinot, P., Lortat-Jacob, H., and Herbomel, P. (2012). Inflammatory chemokines direct and restrict leukocyte migration within live tissues as glycan-bound gradients. Curr. Biol. *22*, 2375–2382.

Schwitalla, S., Fingerle, A.A., Cammareri, P., Nebelsiek, T., Göktuna, S.I., Ziegler, P.K., Canli, O., Heijmans, J., Huels, D.J., Moreaux, G., et al. (2013). Intestinal tumorigenesis initiated by dedifferentiation and acquisition of stem-cell-like properties. Cell *152*, 25–38.

Shimozono, S., Iimura, T., Kitaguchi, T., Higashijima, S., and Miyawaki, A. (2013). Visualization of an endogenous retinoic acid gradient across embryonic development. Nature *496*, 363–366.

Silver, A.F., and Chase, H.B. (1970). DNA synthesis in the adult hair germ during dormancy (telogen) and activation (early anagen). Dev. Biol. *21*, 440–451.

Stenn, K.S., and Paus, R. (2001). Controls of hair follicle cycling. Physiol. Rev. *81*, 449–494.

Suzuki, N., Hirata, M., and Kondo, S. (2003). Traveling stripes on the skin of a mutant mouse. Proc. Natl. Acad. Sci. USA *100*, 9680–9685.

Teleman, A.A., and Cohen, S.M. (2000). DPP gradient formation in the Drosophila wing imaginal disc. Cell *103*, 971–980.

Visscher, P.K. (2007). Group decision making in nest-site selection among social insects. Annu. Rev. Entomol. *52*, 255–275.

Weber, M., Hauschild, R., Schwarz, J., Moussion, C., de Vries, I., Legler, D.F., Luther, S.A., Bollenbach, T., and Sixt, M. (2013). Interstitial dendritic cell guidance by haptotactic chemokine gradients. Science *339*, 328–332.

Willenborg, S., Lucas, T., van Loo, G., Knipper, J.A., Krieg, T., Haase, I., Brachvogel, B., Hammerschmidt, M., Nagy, A., Ferrara, N., et al. (2012). CCR2 recruits an inflammatory macrophage subpopulation critical for angiogenesis in tissue repair. Blood *120*, 613–625.

Youk, H., and Lim, W.A. (2014). Secreting and sensing the same molecule allows cells to achieve versatile social behaviors. Science *343*, 1242782.

A

Hairs plucked	Diameter of plucked area, mm	Plucking area,mm^2	Plucking density hairs per mm^2	Number of regenerated hairs	Density of regenerated hairs per mm^2
200	2.4	4.50	44.44	237.7	52.50
200	3.0	7.10	28.17	452.0	63.90
200	4.0	12.60	15.87	776.8	61.80
200	5.0	19.60	10.20	1276.0	65.00
200	6.0	28.30	7.07		
200	7.0	38.50	5.19		
200	8.0	50.30	3.98		

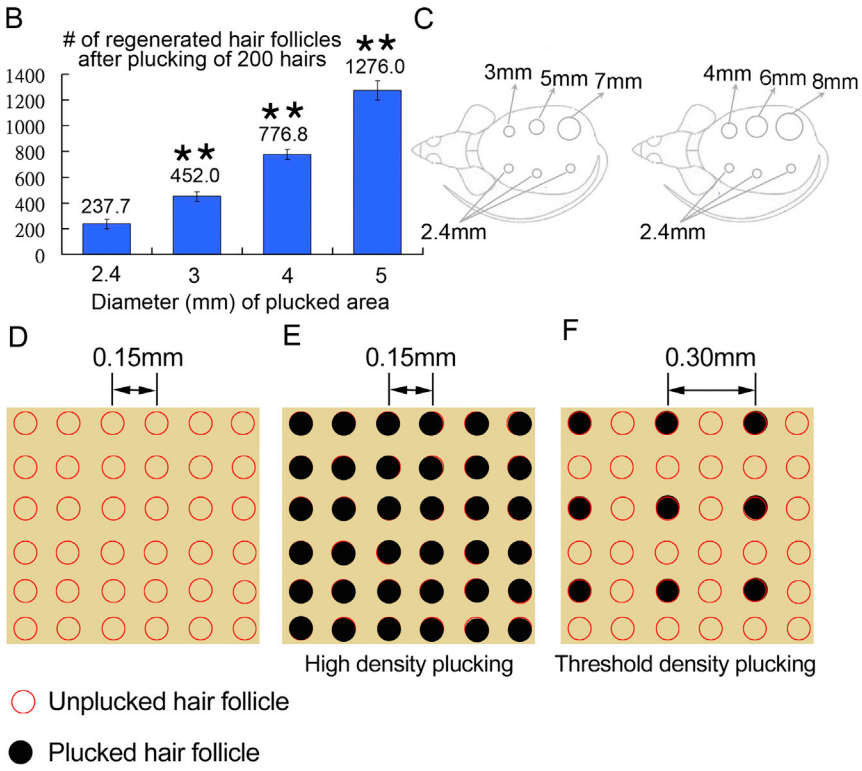

Figure S1. Threshold Response of Regeneration after Quantitative Plucking, Related to Figure 1

(A) Table showing the density of plucked hair and the regenerative response.

(B) The total number of follicles that regenerated from plucked areas of 4.5, 7.1, 12.6, and 19.6 mm^2 was 237.7, 452, 776.8, and 1,276, respectively.

(C) Schematic illustration of quantitative hair plucking design. Two hundred hairs were plucked from each circular area, ranging from 2.4 to 8 mm in diameter (quantitative hair plucking). Plucked regions are encircled with a marker pen. The 200 hairs were evenly spaced within the circle area, then the plucking density of 2.4, 3, 4, 5, 6, 7, and 8 mm in diameter will be 44.44, 28.17, 15.87, 10.20, 7.07, 5.19, and 3.98 hairs/mm^2, independently.

(D) Normal hair density in adult mouse is about 44.44 hairs/mm^2. The distance between each hair follicle is ~0.15 mm.

(E) When we plucked the hair follicles in high density (thus 200 hairs occupy ~4.5 mm^2 of skin surface [area = 2.4 mm in diameter; area = $\pi \times$ radius^2]), all the hairs within this area will be plucked and the distance between plucked hair follicles will be 0.15 mm.

(F) When we plucked the hair follicles in threshold density (200 hairs from the circle with 5 mm in diameter), only 25% of the total hairs within this area will be plucked and the distance between plucked hair follicles will be 0.30 mm. Data are represented as mean ± SD. **$p < 0.001$.

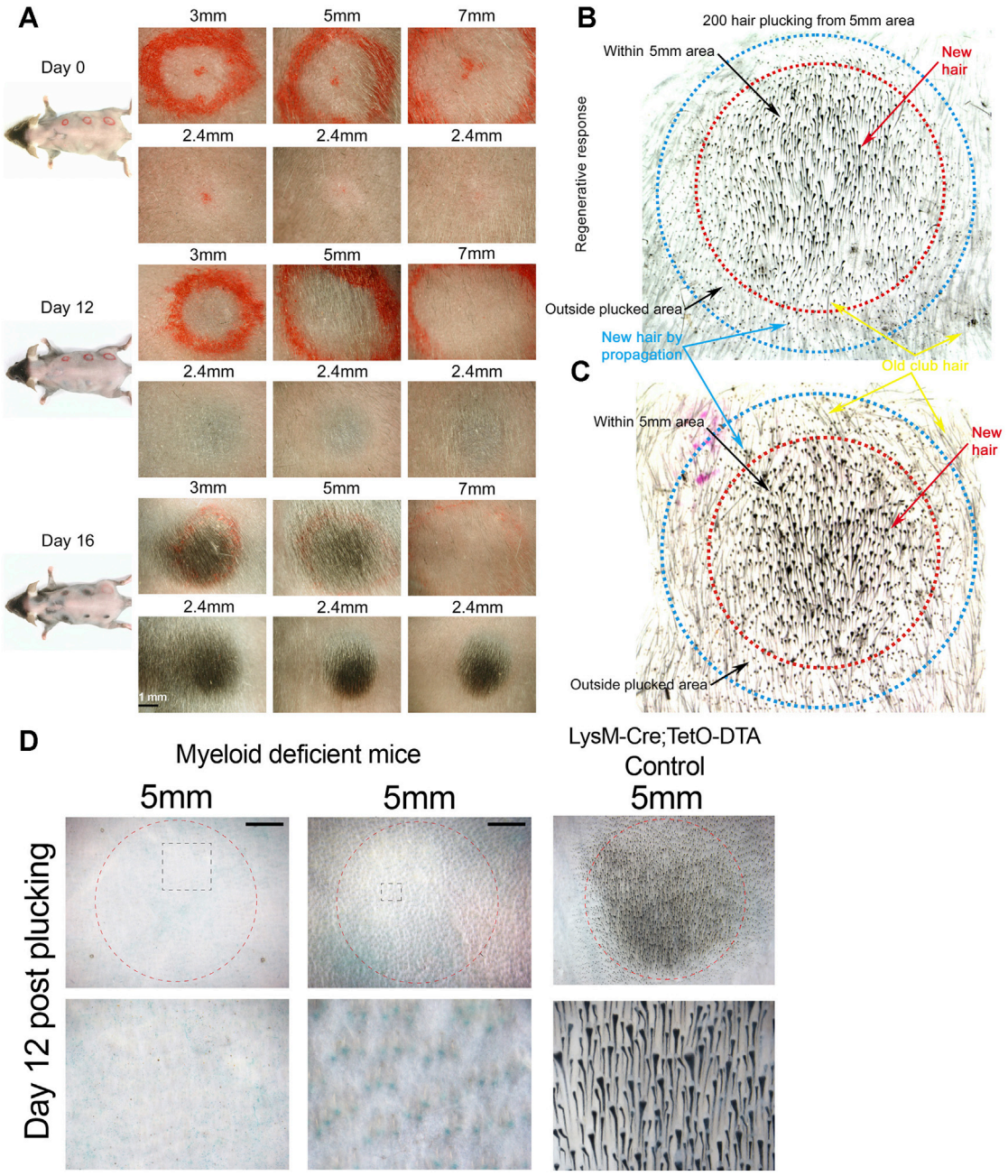

Figure S2. Time Course of Hair Regeneration following Density-Dependent Plucking, Related to Figure 1

(A) Two hundred hairs were plucked from different sized circular regions (2.4, 3, 5, and 7 mm diameter, respectively). When the plucked area was <5 mm in diameter, all the hair follicles within this area entered anagen simultaneously, and the anagen wave also propagated outside the boundaries of the plucked area.

(B) Detail of regenerating region. High-magnification view of regenerative response to plucking involves the regeneration of all follicles (the 200 plucked and 600 unplucked) within the plucked area (dotted red circle).

(C) This is followed by regeneration of unplucked follicles (400 HFs in total) outside the boundaries of the plucked area due to hair wave propagation (dotted blue circle).

(D) Two replicate samples demonstrate that myeloid deficient mouse hair follicles do not regenerate like control samples in response to the plucking of 200 hairs within a 5 mm diameter circle.

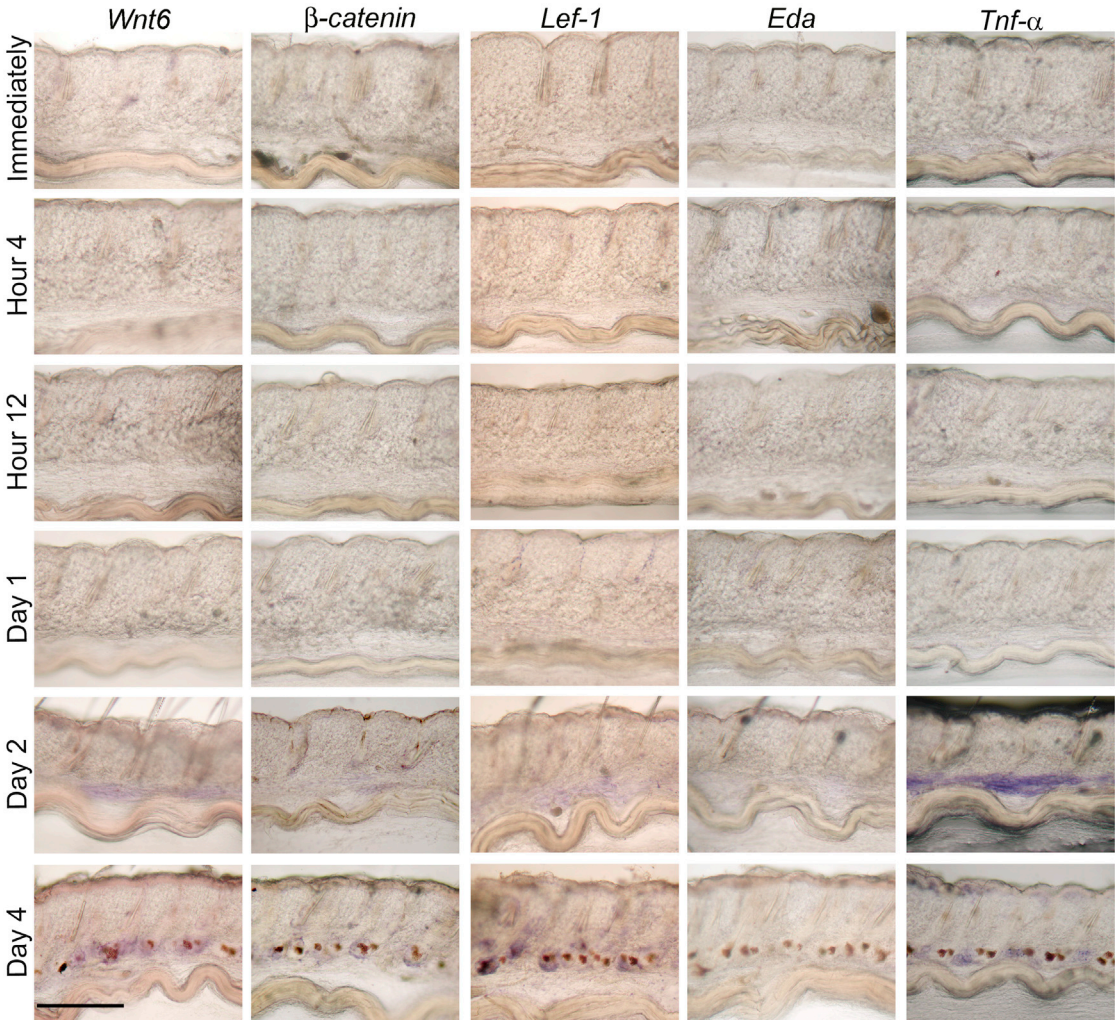

Figure S3. Endogenous Expression Pattern of Wnt Signaling Pathway and Eda at Different Time Points after Plucking, Related to Figure 3

Whole mount in situ hybridization of skin strips (Plikus et al., 2008) show Wnt6, Lef-1 and β-catenin are upregulated within new anagen follicles four days after wax stripping and expression is retained throughout the anagen phase. The expression of Eda continues during anagen phase and is restricted inside the hair follicles without any extra-follicular distribution. Tnf-α is upregulated in the inter-follicular area beginning two days after wax stripping.

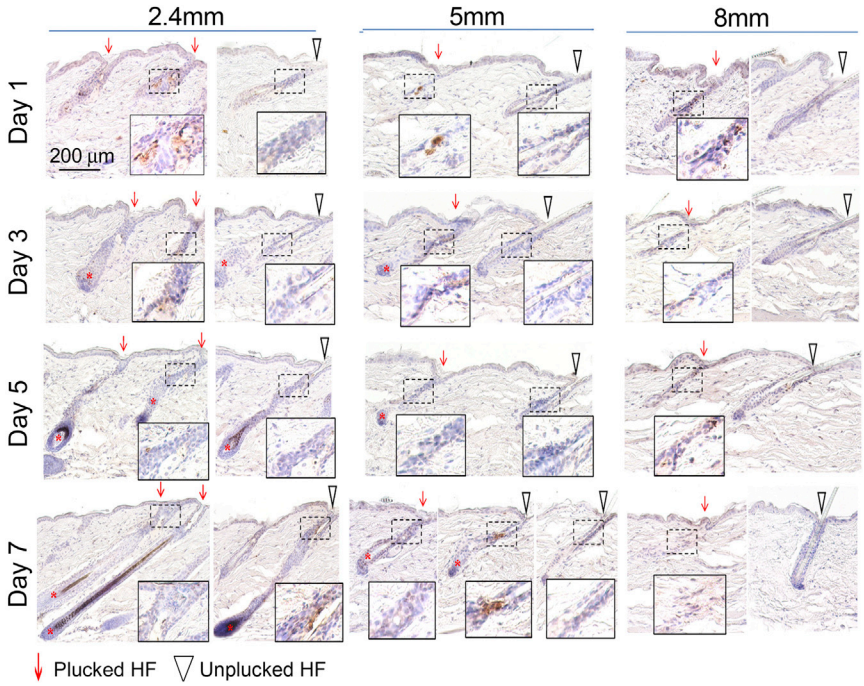

Figure S4. Plucking-Induced Apoptosis in HF Cells, with Peak at Day 1, Related to Figure 3

TUNEL staining on quantitative plucking samples demonstrates that apoptosis only occurs in plucked HFs and the percentage of apoptotic cells is proportional to plucking density (Red arrow: plucked hair follicle; white arrow head: unplucked hair follicle). Areas in the dotted boxes are enlarged in the insets. Red asterisks indicate regenerating HFs.

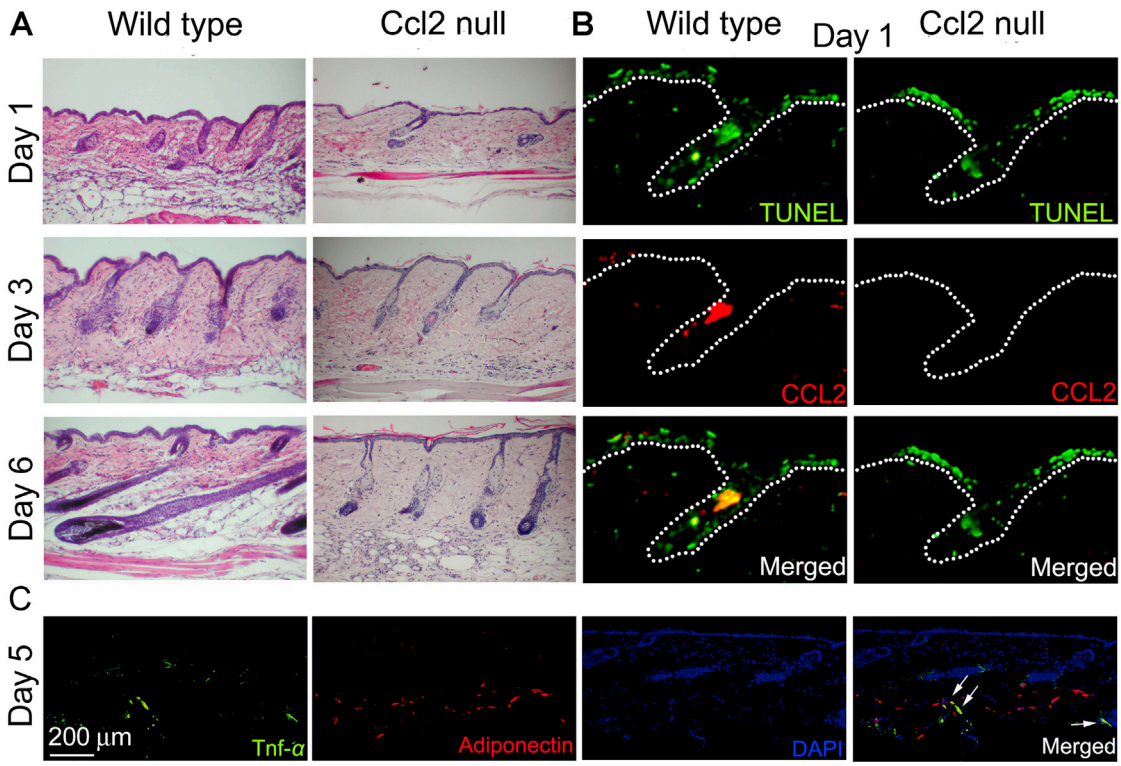

Figure S5. CCL2 Is Involved in Plucking Induced Hair Regeneration, and Tnf-α Is Partially Released by the Adipocyte Layer, Related to Figure 4

(A) Hair re-growth is retarded when whole back skin was waxed from CCL2 null mice. In wild-type mice HFs start to proliferate 3 days after waxing and regenerate to anagen VI by 6 days. In contrast, CCL2 null mouse HFs remain in telogen 3 days after waxing, and are still at anagen III to IV at day 6.

(B) CCL2 null mice show similar apoptotic HF cells following plucking compared with wild-type mice, but do not induce CCL2 in apoptotic HF cells as determined by immunostaining.

(C) Immunostaining shows a small amount of Tnf-α expression is contributed by inter-follicular adipocytes.

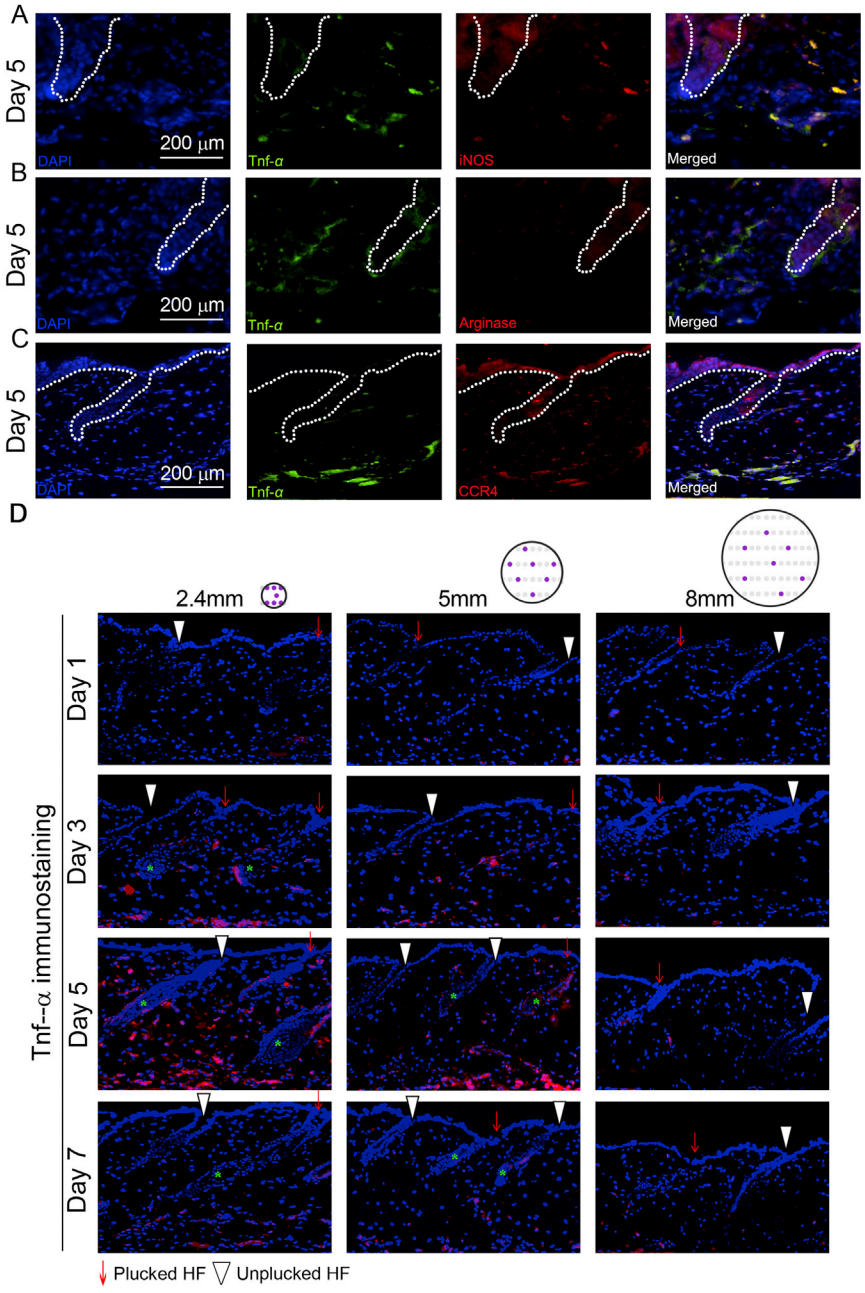

Figure S6. CCR4 (+) M1 Macrophage Are Recruited to the Plucking Field, and the Expression Level of Tnf-α Is Proportional to the Plucking Density, Related to Figures 5 and 6

(A) M1 marker iNOS staining showed that Tnf-α is mainly produced by M1 macrophages.

(B) M2 marker arginase staining is negative in Tnf-α (+) macrophages.

(C) Tnf-α (+) macrophages express CCR4.

(D) Immunostaining shows Tnf-α (+) cells (pink) are attracted to plucked (red arrows) and neighboring unplucked (white arrowheads) follicles in the 2.4mm and 5mm groups, but not in the 8mm group. The circle with purple dots indicates the topology of plucked follicles (please also see Figure 1F). In the 5mm group (Day 5), the regenerating follicles (green asterisks) were only observed within the high-Tnf-α zone induced by follicle plucking.

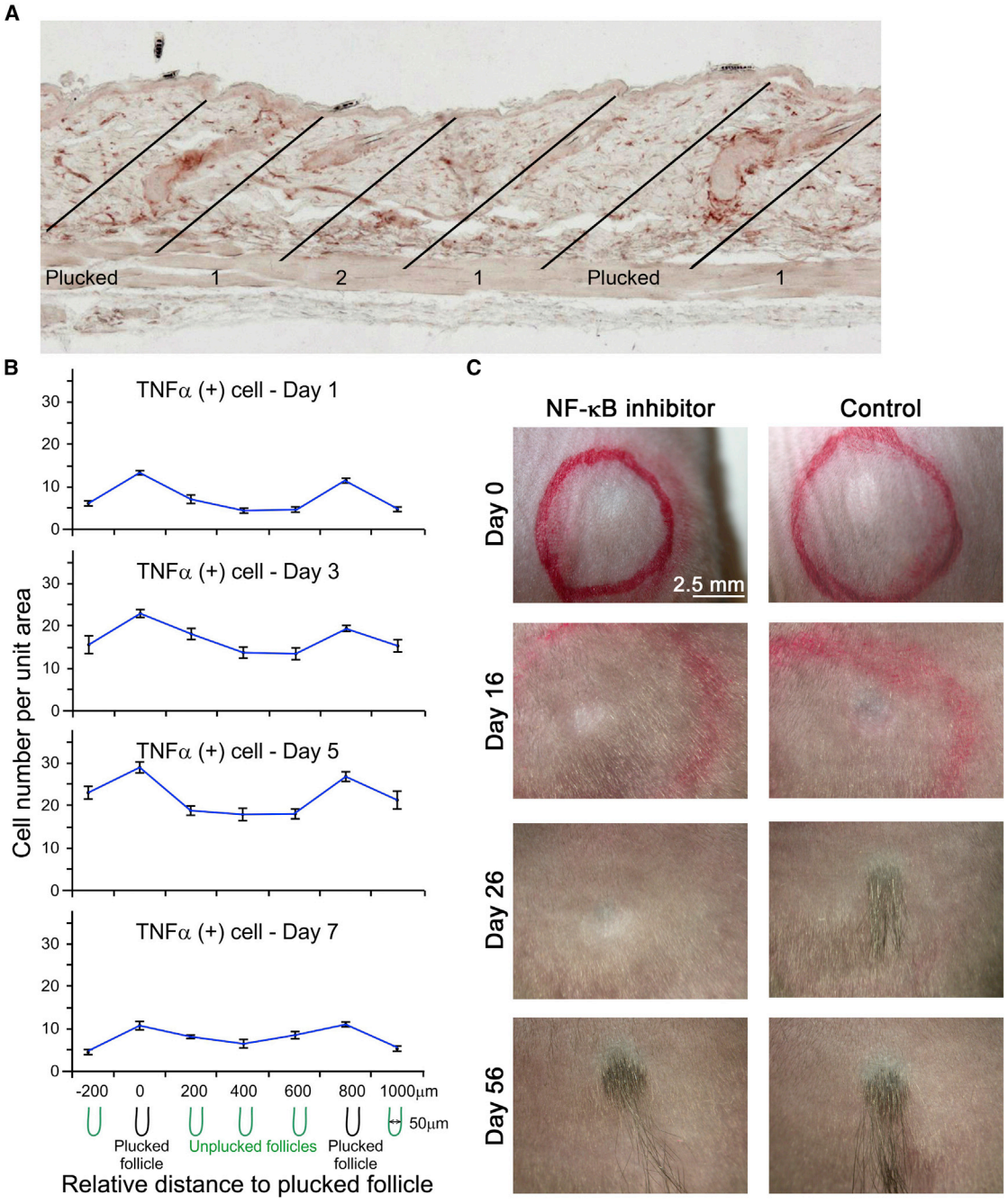

Figure S7. Shift of Tnf-α-Positive Cells at Different Days after Plucking and NF-κB Involves in Plucking-Induced Hair Regeneration, Related to Figures 5 and 6

(A) Method to count of F4/80 macrophages and Tnf-α positive cells. 200 μm segments are marked by using a metered eyepiece. The number of positive cells in the area are counted. The unit area are purposefully aligned to be parallel to the axis of the hair follicle. 3 sections were counted.

(B) The number of Tnf-α positive cells in relation to their distance from plucked hair follicles are quantified. At day 1, Tnf-α positive cells are close to the plucked hair follicles, but some are also seen in the inter-plucked dermis. In day 3 and 5, there are more macrophages distributed in the inter-plucked follicle dermis, making a more even distribution. The response reaches its maximum at 5 days and falls off at day 7. Plucked (black) and unplucked (green) follicles are show schematically beneath the plots. (Data are represented as mean ± SD).

(C) Subcutaneous injection of NF-κB inhibitor can delay plucking-induced hair regeneration by 10 days when 200 hairs were plucked in high density.